Received: 1 August 2022 | Revised: 3 April 2023 | Accepted: 20 April 2023

DOI: 10.1111/1541-4337.13169

COMPREHENSIVE REVIEW

Comprehensive REVIEWS in Food Science and Food Safety WILEY

Aggregates-based fluorescence sensing technology for food hazard detection: Principles, improvement strategies, and applications

Zhuoyun Chen[1,2,3] | **Ji Ma**[1,2,3,4] | **Da-Wen Sun**[1,2,3,5]

[1]School of Food Science and Engineering, South China University of Technology, Guangzhou, China

[2]Academy of Contemporary Food Engineering, South China University of Technology, Guangzhou Higher Education Mega Centre, Guangzhou, China

[3]Engineering and Technological Research Centre of Guangdong Province on Intelligent Sensing and Process Control of Cold Chain Foods, & Guangdong Province Engineering Laboratory for Intelligent Cold Chain Logistics Equipment for Agricultural Products, Guangzhou Higher Education Mega Centre, Guangzhou, China

[4]State Key Laboratory of Luminescent Materials and Devices, Center for Aggregation-Induced Emission, South China University of Technology, Guangzhou, China

[5]Food Refrigeration and Computerized Food Technology (FRCFT), Agriculture and Food Science Centre, University College Dublin, National University of Ireland, Belfield, Dublin 4, Ireland

Correspondence
Da-Wen Sun, School of Food Science and Engineering, South China University of Technology, Guangzhou 510641, China.
Email: dawen.sun@ucd.ie; URL: http://www.ucd.ie/refrig, http://www.ucd.ie/sun

Funding information
National Natural Science Foundation of China, Grant/Award Number: 3217161084; Guangzhou Key Laboratory for Intelligent Sensing and Quality Control of Agricultural Products, Grant/Award Number: 202102100009; Guangdong Provincial Science and Technology Plan Projects, Grant/Award Number: 2020A1414010160; Guangdong Provincial Science and Technology Plan Projects, Grant/Award Numbers: 2022A1515012489, 2020A1515010936; Contemporary International Collaborative Research Centre of Guangdong Province on Food Innovative Processing and Intelligent Control, Grant/Award Number: 2019A050519001; Common Technical Innovation Team of Guangdong Province on Preservation and Logistics of Agricultural Products, Grant/Award Number: 2023KJ145

Abstract

Aggregates often exhibit modified or completely new properties compared with their molecular elements, making them an extraordinarily advantageous form of materials. The fluorescence signal change characteristics resulting from molecular aggregation endow aggregates with high sensitivity and broad applicability. In molecular aggregates, the photoluminescence properties at the molecular level can be annihilated or elevated, leading to aggregation-causing quenching (ACQ) or aggregation-induced emission (AIE) effects. This change in photoluminescence properties can be intelligently introduced in food hazard detection. Recognition units can combine with the aggregate-based sensor by joining the aggregation process, endowing the sensor with the high specificity of analytes (such as mycotoxins, pathogens, and complex organic molecules). In this review, aggregation mechanisms, structural characteristics of fluorescent materials (including ACQ/AIE-activated), and their applications in food hazard detection (with/without recognition units) are summarized. Because the design of aggregate-based sensors may be influenced by the properties of their components, the sensing mechanisms of different fluorescent materials were described separately. Details of fluorescent materials, including conventional organic dyes, carbon nanomaterials, quantum dots, polymers and polymer-based nanostructures and metal nanoclusters, and recognition units, such as aptamer, antibody,

molecular imprinting, and host–guest recognition, are discussed. In addition, future trends of developing aggregate-based fluorescence sensing technology in monitoring food hazards are also proposed.

KEYWORDS
aggregation, fluorescent sensors, food safety hazard detection, recognition units

1 | INTRODUCTION

The aggregation of molecules plays an important role in determining the function of the molecules. Molecular aggregates are defined as irregular clusters of many molecules. Compared with their molecular elements, aggregates often exhibit modified or completely new properties, making them an extraordinarily advantageous form of materials (Zhang, Zhao, et al., 2020). In particular, the alteration of photoluminescence properties indicates that molecular aggregates can be used for developing new platforms for detection at the molecular level.

On the other hand, in molecular aggregates, the photoluminescence properties or organic chromophores at the molecular level can be annihilated or elevated, and the annihilation phenomenon is defined as the aggregation-causing quenching (ACQ) effect, whereas the elevation phenomenon is termed the aggregation-induced emission (AIE) effect. Figure 1 shows the mechanisms and phenomena of ACQ and AIE effects. In these phenomena, the ACQ effect is common for most aromatic hydrocarbons and their derivatives, whereas the AIE effect was discovered when Tang et al. (2001) found that silole compounds were thoroughly nonluminescent in solution but had high emissivity as nanoscale aggregates. The mechanism of the ACQ effect can be summarized as an increasing number of aromatic rings melding together with aggregation, leading to bigger discotic plates and subsequently an increased chance of such large luminophores forming excimers or exciplexes (Zhang, Zhuo, et al., 2019). However, the mechanism of the AIE effect can be interpreted as the restriction of intramolecular motion that inhibits nonradiative decay and the opening up of the radiative channel that leads to increases in emission (Hong et al., 2011). Both ACQ and AIE effects possess inherent advantages in the construction of fluorescence sensors. To be specific, AIE luminogens (AIEgens) exhibit excellent photostability, and rich and strong photoluminescence properties, making AIE-based fluorescence sensors helpful in rapid, trace, and in situ detection (Wang et al., 2021; Wu et al., 2020; Xie et al., 2020). In the meantime, ACQ-based fluorescence sensors are useful tools for food hazard detection because of their excellent recognition function and low-cost synthesis route (Li, Wang, et al., 2021).

Generally speaking, molecular aggregation often occurs in both organic and inorganic luminophore systems. Fluorescent materials, including organic molecules, carbon nanomaterials, quantum dots (QDs), polymers and polymer-based nanostructures, and metal nanoclusters (MNCs), possess the potential to form into aggregate (Su et al., 2021). Due to the changes in fluorescence properties, these aggregates can be applied for designing sensors with high sensitivity to detect corresponding analytes through various strategies. However, in aggregating fluorescent materials, analytes with similar structures such as with the same functional groups or electronegativity can stimulate the aggregation of the same material, which lowers the selectivity of aggregate-based fluorescence sensors, preventing them from wider applications (Huang, Guo, et al., 2020). Introducing recognition units, such as aptamer, antibody, molecular imprinting, and host–guest, into the aggregate-based sensors would significantly improve the selectivity and specificity (Capoferri et al., 2018; Huang, Guo, et al., 2020), and therefore, many studies have thus been conducted in this area (Guo et al., 2020; Wang, Zheng, et al., 2019; Zhang, Duan, et al., 2020).

Food safety is a global concern that covers many different areas of our everyday life, and rapid and reliable detection of food hazards is thus an important food safety issue in the food industry (He, Sun, Wu, Pu, & Wei, 2022; Zhang, Huang, Pu, & Sun, 2021). Aggregating fluorescent materials have thus been utilized to monitor the safety hazards in food (Chen et al., 2020; Ling et al., 2020). Huang, Guo et al. (2020) summarized the development of AIEgens for food safety hazard supervising systems, focusing on the sensing strategies and effect of AIEgens on different types of food contaminations, whereas Wan et al. (2021) reviewed the applications of AIE materials for detecting various kinds of toxic ions in water. Sargazi et al. (2022) provided a review of fluorescent nanosensors for the detection of a variety of biological macromolecules. However, these reviews paid more attention to the target analytes instead of the fluorescent materials that participated in sensing systems. There is a knowledge gap for the aggregation behaviors, related principles, and structural features

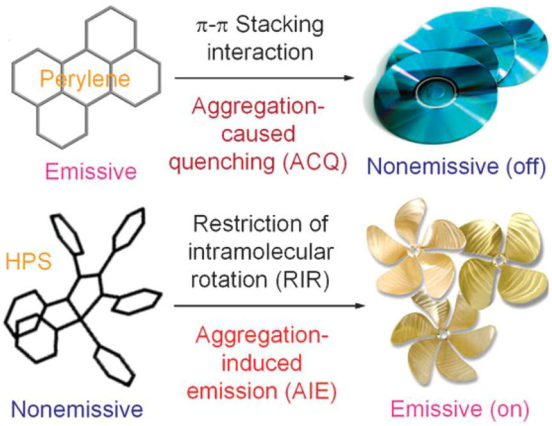

FIGURE 1 General mechanisms of aggregation-caused quenching (ACQ) and aggregation-induced emission (AIE).

of each fluorescent material to provide useful guidance for researchers. In the meantime, although the application of organic AIEgens has been comprehensively reviewed (Gao & Tang, 2017), Liu et al. (2018) summarized the aggregation of gold-nanoparticle and the application in colorimetric food safety monitoring, and Ma et al. (2015) made the comparison between ACQ and AIE active molecules by their structure and fluorescence difference. Up to now, research on the application of the ACQ phenomenon to develop fluorescent sensors is still insufficient. No review is available making the comprehensive summary of both advanced ACQ- and AIE-active organic and nanomaterials applied in food hazard detection and corresponding aggregation mechanisms with/without recognition units. Therefore, the purpose of the current review is to summarize and compare recently available publications on the topic. In this review, aggregation mechanisms and structural characteristics of ACQ/AIE-activated fluorescent materials (including organic dyes, carbon nanomaterials, QDs, polymers and polymer-based nanostructures, and MNCs) are summarized, respectively. The principles of different recognition units (aptamer, antibody, molecular imprinting, and host–guest recognition) participating in aggregate-based sensors are depicted. The application and effectiveness of ACQ/AIE-based sensors in foodborne or food-related hazard detection (with/without recognition units) are discussed. In addition, improvement strategies and future trends of developing aggregate-based fluorescence sensing technology in monitoring food hazards are proposed. Scheme 1 shows the principle, improvement, and application of aggregate-based fluorescence sensing technology for food hazard detection. It is expected that this review would arouse more research interests and applications in aggregate-based sensors for food safety and quality control.

2 | AGGREGATION AND AGGREGATES

In fluorescent materials, aggregation normally leads to a decline or increase of their photoluminescence properties at the molecular level; therefore, these aggregates are divided into those with ACQ effects and those with AIE effects (Zhang, Duan, et al., 2020). These effects can therefore be used for applications in the detection of foodborne or food-related safety hazards without the need of combining with recognition units.

2.1 | Aggregates with aggregation-caused quenching effects

The quenching effects of the aggregates are due to the increase in the number of aromatic rings melding, leading to the transformation of bigger discotic plates, and such large luminophores are more likely to form excimers or exciplexes, causing fluorescence quenching (Zhang, Duan, et al., 2020). According to the molecular composition, aggregates with the ACQ effect can be classified into carbon nanomaterials, MNCs, QDs, polymers, and polymer-based nanostructures.

2.1.1 | Carbon nanomaterials

Many carbon nanomaterials with the ACQ effect are available, and those that can be used for constructing ACQ-based sensing systems for food-related safety hazards include carbon dots (CDs), graphene QDs (GQDs) and oxidizing two-dimensional titanium carbide (Ti_3C_2 MXene) nanosheets (Desai et al., 2019; Wu & Tong, 2019).

CDs can be defined as spherical-like carbon particles (graphitic fragments) with sizes less than 10 nm, which exhibit some merits for detection application, such as abundant external functional groups, special molecular recognition ability, rich and strong photoluminescence properties, and enjoyable water solubility (Li, Shi, et al., 2021). Construction of multicomponent detection based on CDs without tedious surface modification is always a challenging task (Wu & Tong, 2019). This challenge can be overcome by introducing the ACQ phenomenon in CDs-based detection. Wu and Tong (2019) fabricated nitrogen- and sulfur-codoped CDs for Hg^{2+} and sulfide multicomponent detection on the account of the ACQ phenomenon, exhibiting good linearity (R^2 = 0.996) between fluorescence intensity and the concentration in the range of 0.5–50 μmol/L (Figure 2a). The bright blue fluorescence of N,S-CD solution would be quenched upon the addition of Hg^{2+} because it will be coordinated with the surface oxygen-containing groups of N,S-CDs to form

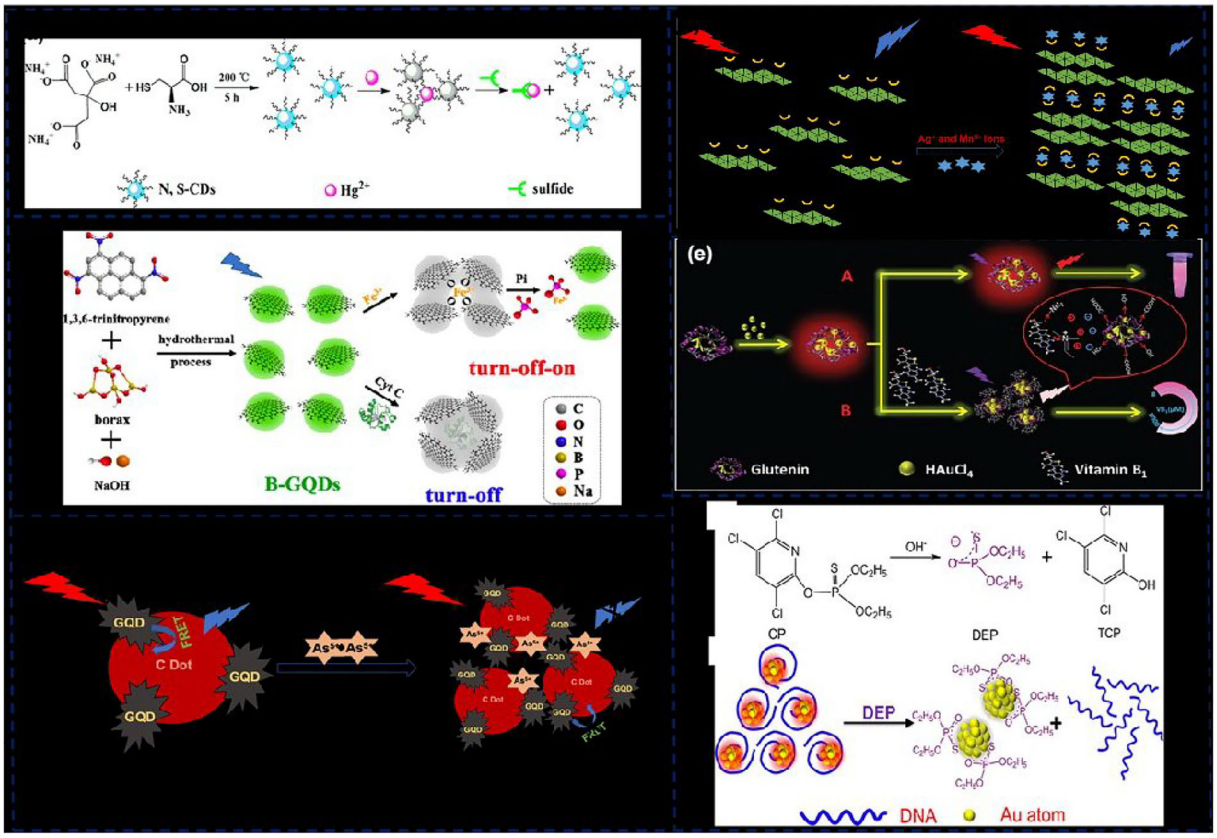

FIGURE 2 (a) Nitrogen- and sulfur-codoped carbon dots (CDs) for Hg^{2+} detection (Wu & Tong, 2019); (b) high-quality aggregation-causing quenching (ACQ) boron-doped graphene quantum dots (GQDs) for Fe^{3+} detection (Ge et al., 2019); (c) an ACQ sensor of GQDs and CDs for As^{5+} detection (Chini et al., 2019); (d) selective sensing of metal ions (Ag^{+}, Mn^{2+}) using Ti_3C_2 MXene nanosheets (Desai et al., 2019); (e) glutenin-directed gold nanoclusters for Vitamin B1 detection (Liu, Gan, et al., 2020); (f) non-sulfated DNA templates of Au nanoclusters (AuNCs) for organophosphorus pesticides (OPs) detection (Lu et al., 2018).

complexes, promoting the electron transfer from CDs to Hg^{2+}. However, this aggregation would be destroyed by sulfide, leading to fluorescence recovery. As a subgroup of CDs, GQDs are regarded as potential candidates for sensor application due to high stability, hypotoxicity, and high solubility in various solutions, which can be obtained by converting graphene sheets into zero-dimension. Zeng, Zhu, & Sun, 2022; Chini et al. (2019) combined GQDs and CDs to build an ACQ sensor for Hg^{2+} and As^{5+} (Figure 2c) because the spectral overlap between the GQDs emission profile and CDs absorption profile makes them a fluorescence resonance energy transfer (FRET) pair. As^{5+} could promote the aggregation of GQDs and CDs through the strong affinity of As^{5+} toward the carboxylic group, shortening the distance between GQDs and CDs, the Dexter process described as collisional quenching phenomenon decreased the FRET fluorescence signal of the complexes.

However, the photochemical properties of CDs and GQDs are not as good as QDs (CdSe and CdTe), limiting their application in microscale detection (Wei et al., 2019). Researchers are devoted to seeking the preparation of nanocrystals with enhanced properties. Ti_3C_2 MXene belongs to the family of 2D transition metal carbides or nitrides with a series of fascinating properties, such as surface hydrophilicity and rich surface chemistry, which is considered to be an excellent candidate for fluorescence sensors (Desai et al., 2019). Construction of MXene-based sensors is still in a budding phase requiring research attention to widen their applications. Desai et al. (2019) used Ti_3C_2 MXene nanosheets to develop ACQ-based sensing systems for selective sensing of metal ion Ag^{+}, exhibiting a low detection limit of 9.7 nmol/L (Figure 2d). The aggregation of Ti_3C_2 MXene nanosheets was triggered by the strong interaction between Ag^{+} ions and Ti_3C_2 nanosheet surface functional groups (–OH, O^{-}, and F^{-}), leading to the decrease in fluorescence intensity.

All in all, it can be concluded that the aggregation of carbon nanomaterials is usually induced by electrostatic interaction between metal ions and materials surface functional groups, whereas the quenching is due to the promotion of electron transfer or decrease of FRET via collisional quenching phenomenon.

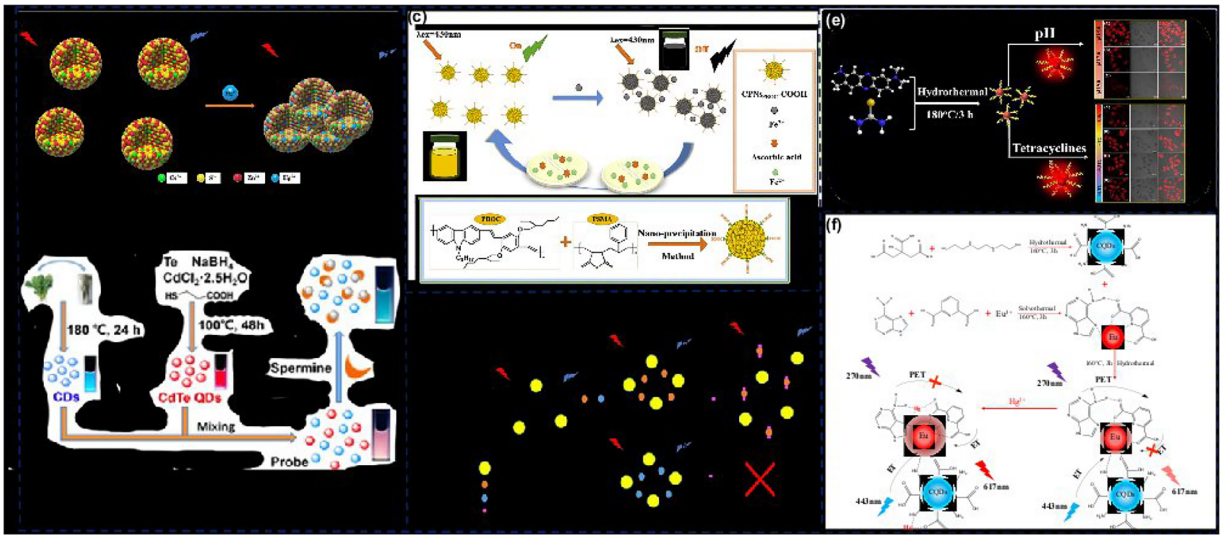

FIGURE 3 (a) A double-emission ratiometric ZnS:Ce quantum dots (QDs) fluorescence sensor (Chu et al., 2020); (b) dual-emission ratiometric fluorometric probe of CdTe QDs and carbon dots (CDs) (Fu et al., 2020); (c) conjugated polymer nanoparticles with carboxyl groups for ascorbic acid detection (Wang, Zhang, et al., 2020); (d) poly[(9,9-dioctylfluorenyl-2,7-diyl)-alt-*co*-(1,4-benzo-(2,1′,3)-thiadiazole)] (PFBT) polymer dots functionalized by –COOH groups for Cu^{2+} or Fe^{3+} and histamine detection (Chabok et al., 2019); (e) a "turn-on" red fluorescent CDs for tetracyclines detection (Li, Chen, et al., 2021; Li, Wang, et al., 2021; Li, Shi, et al., 2021; Li, Xi, et al., 2021); (f) CDs-based dual-emission sensor for Hg^{2+} detection (Gan et al., 2021).

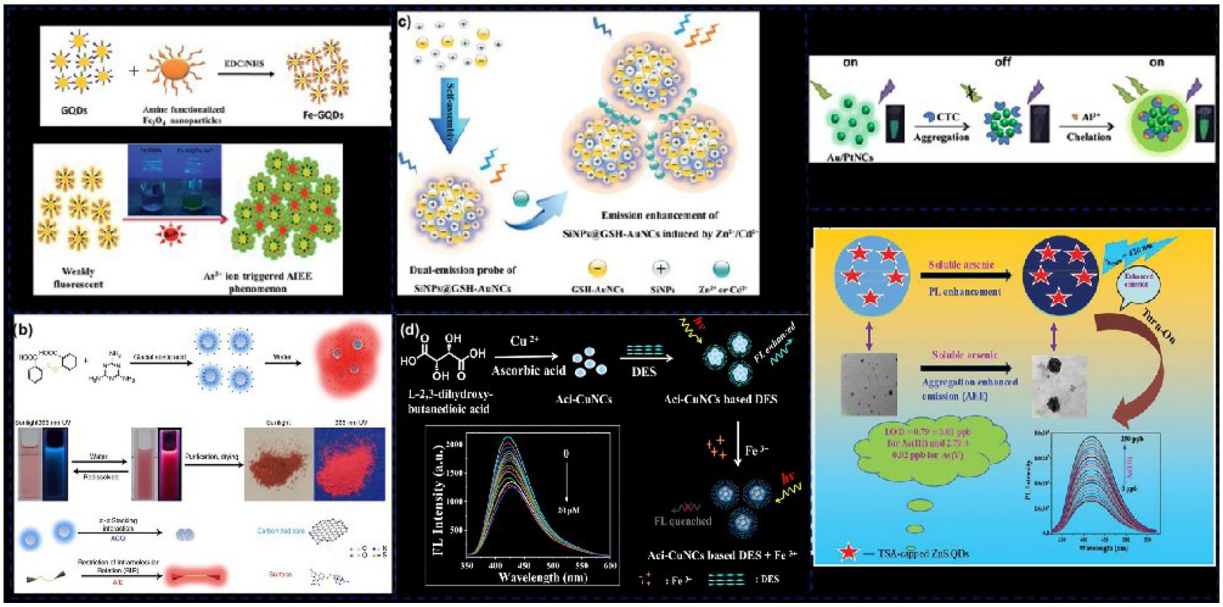

FIGURE 4 (a) An Fe-GQDs fluorescence sensor for arsenic detection (Pathan et al., 2019); (b) hydrophobic carbon dots (CDs) with blue dispersed emission and red aggregation-induced emission (AIE) (Yang et al., 2019); (c) dual-emissive silicon nanoparticles (SiNPs) and glutathione (GSH)–AuNCs self-assembly for Zr^{2+} or Cd^{2+} detection (Qu, Huang, et al., 2018; Qu, Zhao, et al., 2018); (d) a fluorescence sensor for Fe^{3+} based on acid-CuNCs in a deep eutectic solvent medium (Chen, Wang, et al., 2021; Chen, Cheng, et al., 2021); (e) green-emitting Au/Pt NCs capped with polyethyleneimine for chlortetracycline detection (Xu, Meng, et al., 2018); (f) thiosalicylic acid–capped ZnS QDs for total arsenic [As(III)+As(V)] detection (Kayal & Halder, 2019).

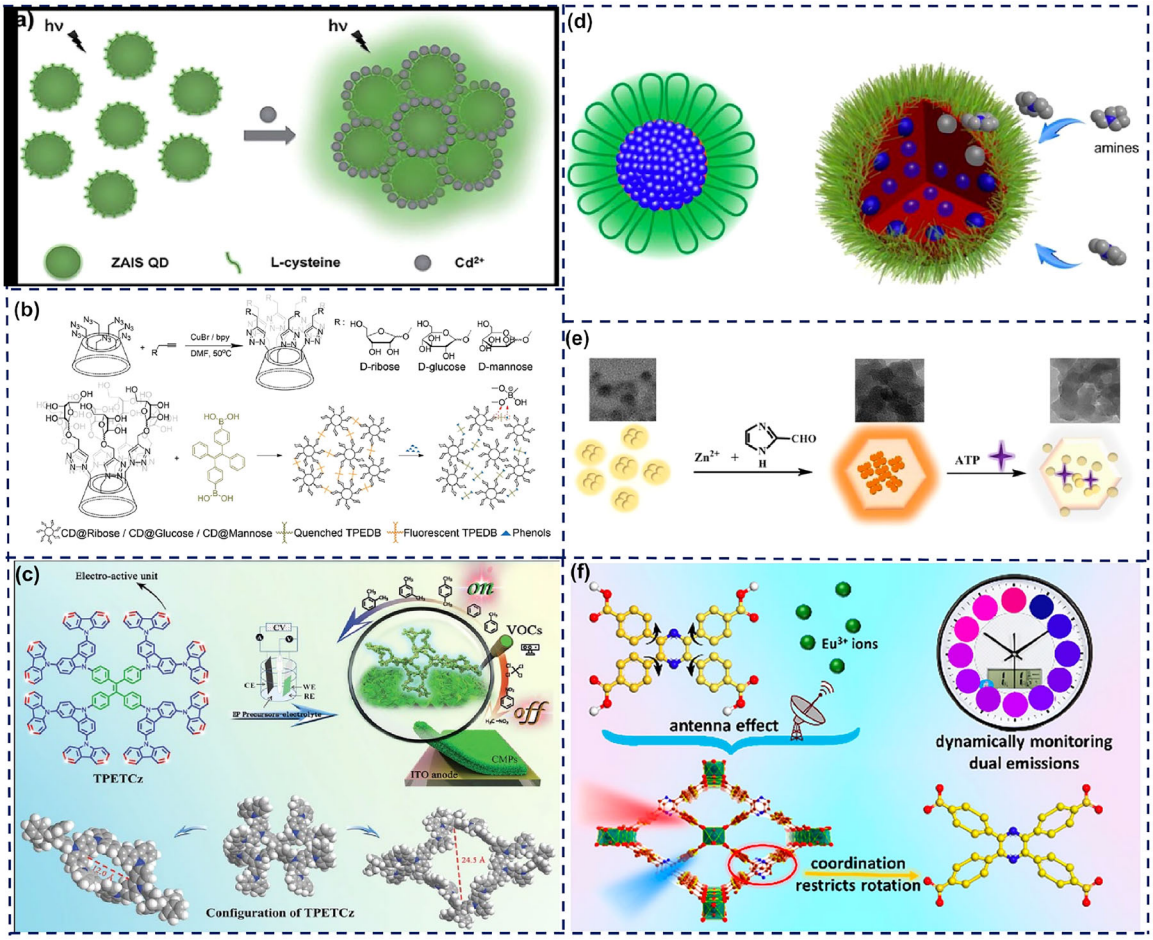

FIGURE 5 (a) L-Cysteine-capped aqueous Zn–Ag–In–S QDs for Cd^{2+} detection (Wei et al., 2019); (b) a sensor of tetraphenylethylene with two boronic acid units (TPEDB) and glycoclusters for phenols pollutant detection (Li et al., 2020); (c) an aggregation-induced emission (AIE) polymer with tetraphenylethylene (TPE) and carbazole group for volatile organic compounds (VOCs) detection (Liu, Wang, et al., 2020); (d) hydrophobic polymers and TPE moiety organized into cores with the AIE effect for aromatic pollutants detection (Zhou et al., 2019); (e) composites based on GSH–CuNCs, Al^{3+} and a zeolitic imidazole framework (ZIF)-90 for adenosine triphosphate (ATP) detection (Gao et al., 2020); (f) metal–organic framework (MOFs) with an AIE ligand and Ln^{3+} ions for arginine detection (Yin et al., 2019).

2.1.2 | Metal nanoclusters

MNCs can be regarded as a bridge between the atomic regime and large metal nanoparticles, which can produce electronically separated energy levels and size-dependent fluorescence (Hu, Sun, Pu, & Wei, 2020; Liu, Gan, et al., 2020). Compared with conventional organic dyes and QDs, MNCs got more attention due to their ultrasmall size, excellent photostability, biocompatibility, and ease of synthesis (Chen, Cheng, et al., 2021).

However, the main issue in applying MNCs is their susceptible and easily oxidized surfaces, making them unstable when exposed to air (Gao, Sun, Tian, & Zhu, 2021; Wang, Bai, et al., 2020). Therefore, many studies have focused on developing more stable families of MNCs with diverse atomic specificity using different capping ligands, which is demonstrated in Table 1 (Lu et al., 2018; Mo et al., 2018; Xu, Meng, et al., 2018). Liu, Gan et al. (2020) synthesized glutenin (Glu)-directed Au nanoclusters (AuNCs) with red fluorescence for Vitamin B1 detection and showed that the positively charged Vitamin B1 neutralized the surface negative charges of Glu@AuNCs, leading to the aggregation of AuNCs and subsequently fluorescence quenching (Figure 2e).

Besides the efforts in improving the stability of MNCs with ACQ properties, other studies have sacrificed great stability to fulfill the higher sensitivity of MNCs as ACQ-based sensors for analytes. The strong Au–S interaction could give high stability to sulfated MNCs but limit the sensitivity; therefore, non-sulfate AuNCs can be used, although they are more fragile but sensitive to sulfate-containing analytes due to the weak interaction between MNCs and non-thiolate reagents (Lu et al., 2018). A chemical sensor has been constructed to measure chlorpyrifos using non-sulfated DNA templates of AuNCs (DNA-AuNCs) as optical probes (Figure 2f). By

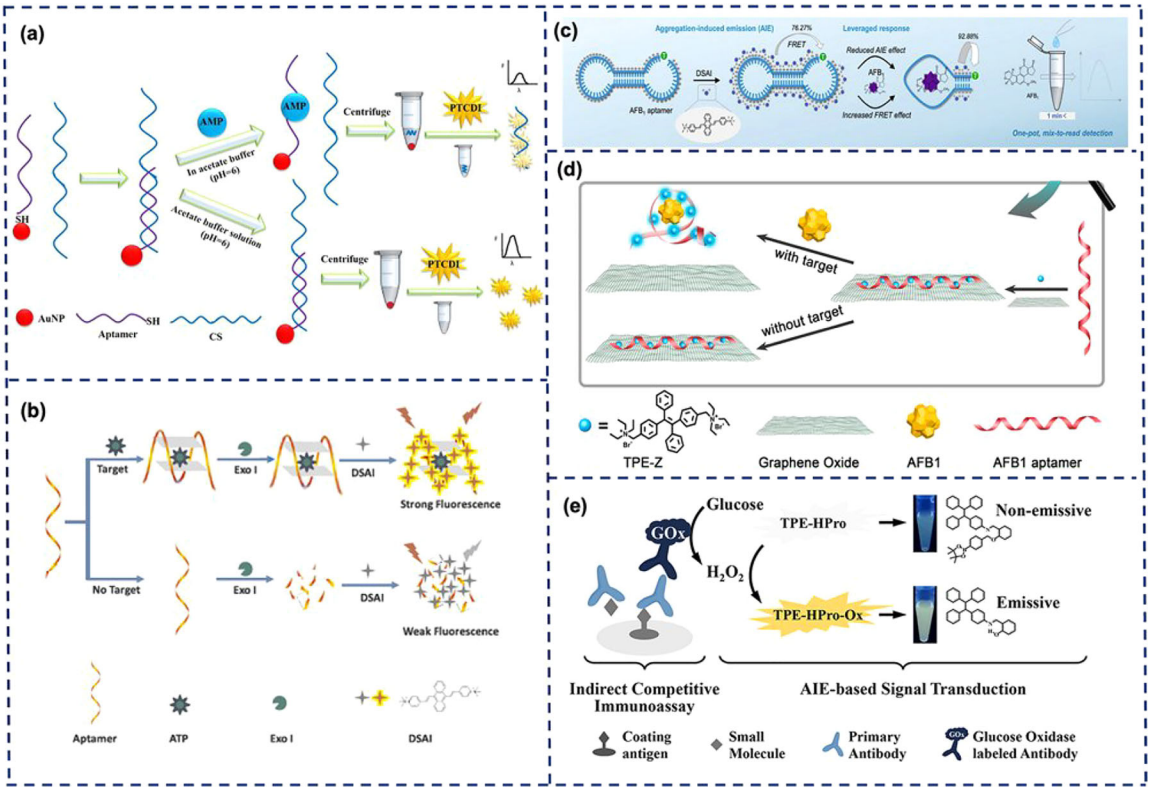

FIGURE 6 (a) AuNP combined with fluorescent aptasensor for selective ampicillin detection (Esmaelpourfarkhani et al., 2020); (b) an aptasensor used 9,10-distyrylanthracene derivative with a short alkyl chain (DSAI) as an aggregation-induced emission luminogen (AIEgen) for adenosine triphosphate (ATP) detection (Li, Guo, et al., 2019); (c) an intrinsic conformation response-leveraged aptamer probe combined with fluorescence resonance energy transfer (FRET) for detecting aflatoxin B_1 (AFB_1) (Zhao, Kong, et al., 2019); (d) an aptasensor of quaternized TPE salt, graphene oxide (GO), and AFB_1 aptamer for AFB_1 detection (Jia, Wu, et al., 2019); (e) a direct enzyme-linked immunosorbent assay (ELISA) platform for generating AIE signals (Yu et al., 2019).

TABLE 1 Summary of ligands has been used for imparting the metal nanoclusters for the aggregation-causing quenching (ACQ) phenomenon.

Nanoclusters	Ligands	Functional groups of ligands	Reference
AuNCs	Inositol	–OH, –COO	Halawa et al. (2018)
AuNCs	Electropositive thiocholine	HS-	Liang and Han (2020)
AuNCs	Glutenins	–COOH, $–NH_2$, –OH, –COO	Liu, Gan et al. (2020)
AuNC	Non-thiolate DNA	Phosphate group	Lu et al. (2018)
AuNCs	DCTX	Reducing sulfhydryl	Ye et al. (2019)
AuNCs	Protamine	–COOH, $–NH_2$	Huang, Zhang et al. (2020)
AuNCs	Nitrogen-doped GQDs	–COOH, $–NH_2$	Su et al. (2021)
AgNCs	Denatured lysozyme	HS–	Mo et al. (2018)
AgNCs	Dihydrolipoic acid	HS–	Ren et al. (2019)
CuNCs	Surfactant-free	–	Sahu et al. (2019)
PtNCs	Chicken egg white	–OH, C=O, C–N	Borse et al. (2020)
Au/PtNCs	Polyethyleneimine	$–NH_2$	Xu, Meng et al. (2018)

Abbreviations: AgNCs, Ag nanocluster; AuNCs, Au nanoclusters; CuNCs, Cu nanoclusters; DCTX, degradation product of cefotaxime sodium; GQDs, graphene quantum dots; GSH, L-glutathione; PtNCs, Pt nanoclusters.

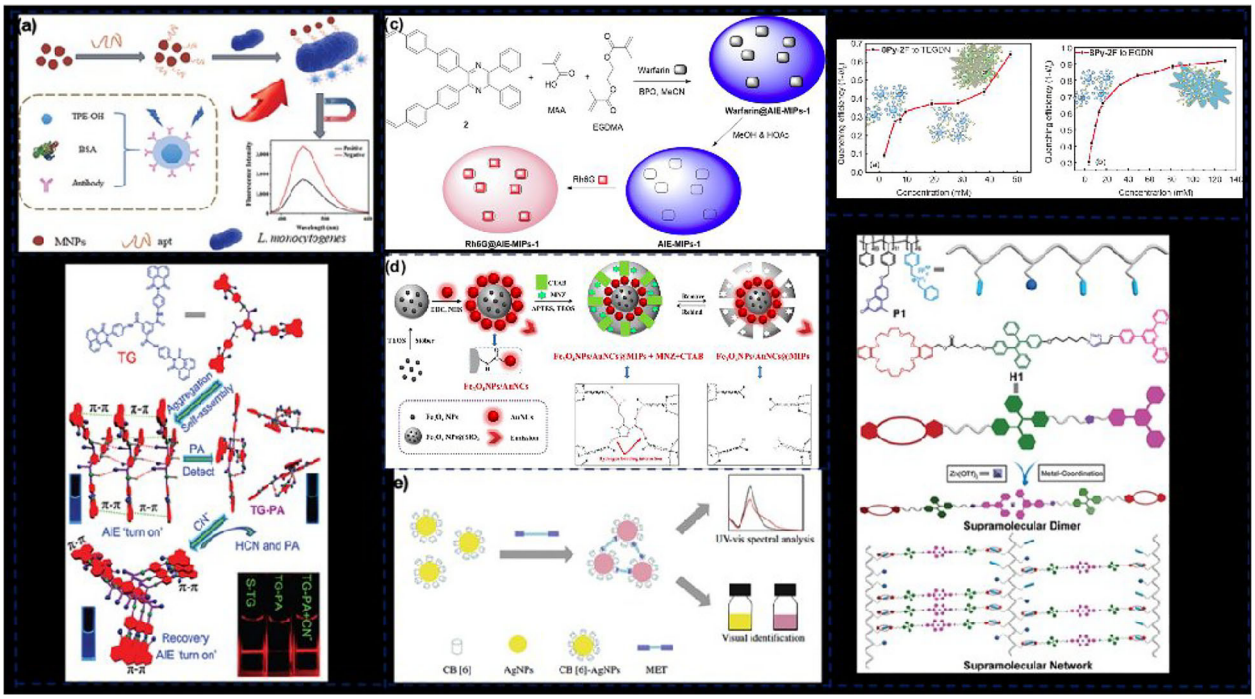

FIGURE 7 (a) Aptamer–magnetic nanoparticles (MNPs) combined with IgG–TPE–OH@ bovine serum albumin (BSA) NPs for *Listeria monocytogenes* detection; (b) a trisnaphthalimide derivative-based supramolecular sensor for detecting picric acid (PA) and CN^- (Lin et al., 2019); (c) tetraphenylpyrazine-based aggregation-induced emission luminogens (AIEgens) combined with molecularly imprinted polymer (MIP) for rhodamine 6G detection (Li, He, et al., 2019); (d) a spherical MIP for metronidazole detection (Tan et al., 2019); (e) an assay of metformin (MET), based on the host–guest molecular recognition of cucurbit[6]uril (CB[6])-AgNPs (Song et al., 2019); (f) multiple anchored fluorene dimers as an aggregate base for dinitrate detection (Jia, Xu, et al., 2019); (g) a coumarin and TPE contained supramolecular network fluorescence sensor for cyclen, Et_3N, and Cl^- detection (Xu, Chen, et al., 2018).

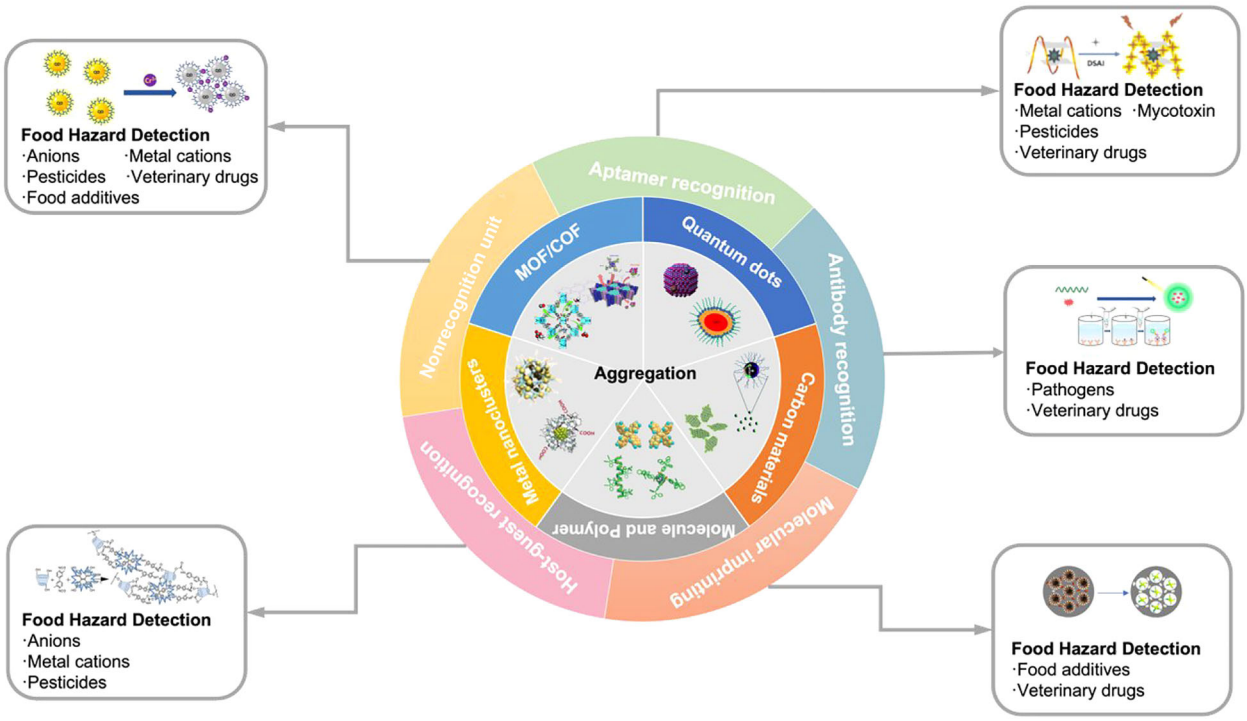

SCHEME 1 The graphical summary of the principle, improvement, and application of aggregate-based fluorescence sensing technology for food hazard detection.

introducing these AuNCs in *S*-contained chlorpyrifos detection, the luminescence AuNCs were remarkably quenched by the chlorpyrifos because of aggregation via synergistic coordination through both Au–S and Au–O atoms, which can be distinguished by the naked eye with a detection limit of 0.50 μmol/L (Lu et al., 2018).

Above all, the aggregation mechanisms of MNCs involve surface negative charges being neutralized or Au–S, Au–O coordination between analytes and MNCs, whereas the quenching effect might be due to the excited electron transfer to the metal via nonradiative decay ways (Li, Xi, et al., 2021).

2.1.3 | Quantum dots

QDs are zero-dimensional semiconductor nanocrystals with strong light absorption, bright narrowband emission across the visible and infrared wavelengths, and tunable surface chemistry (Wei et al., 2019). The ACQ effect helps pave the way to design turn-on/off fluorescent probes with satisfying sensitivity. However, common QDs usually contain hazardous elements in their composition, such as cadmium and lead, causing some safety issues and limiting their application in food matrices. Chu et al. (2020) developed a double-emission ratiometric fluorescence sensor for Hg^{2+} detection by doping ZnS QDs with rare-earth element Ce (ZnS:Ce QDs). After Hg^{2+} addition, ZnS:Ce QDs preferentially absorbed Hg^{2+} to convert some ZnS into more insoluble HgS, thus leading to the aggregation and precipitation of the ZnS:Ce QDs and the transformation of surface structure, followed by fluorescence decline in both two wavelengths (Figure 3a).

In addition, capped ligands, such as organic acid, protein, and thiols, can be used to functionalize QDs to form special sensing abilities (Parani & Oluwafemi, 2020). Chen et al. (2020) used thioglycolic acid to modify CdTe-QDs, achieving specific distinguishment of cereal vinegar, as the hydrogen ions of the vinegar could reduce the charge repulsion and induce aggregation of these QDs, causing fluorescence quenching due to electrons transfer and FRET. More importantly, the aggregation degree of these QDs depended on the concentration of hydrogen ions. Because different organic acids had different abilities to produce hydrogen ions and cause a diverse degree of aggregation, different kinds of cereal vinegar could be specifically distinguished.

Other fluorescence materials can be used to combine with QDs for improving the sensitivity of the detecting systems. Fu et al. (2020) synthesized a dual-emission ratiometric fluorescent probe, composed of CdTe QDs and CDs. The CDs acted as the reference signal, whereas CdTe QDs showed a response to the analyte (spermine), which could be regarded as a spoilage indicator of pork meat through the ACQ effect (Figure 3b). The strong electrostatic interaction and hydrogen bond interaction between CdTe QDs and spermine contributed to the aggregation of CdTe QDs, followed by fluorescence quenching. Introducing CDs in ACQ-active CdTe QDs sensor elevated the sensitivity with the detection limit of 76 nM and generated obvious color change in the presence of spermine.

In general, a variety of analytes can be detected by ACQ-based QDs sensors, including metal ions, biogenic amine, and hydrogen ions, which induce aggregation through neutralization, electrostatic and hydrogen bond interaction, or reducing solubility. In the meantime, the quenching of QDs might be due to electron transfer or the FRET effect.

2.1.4 | Polymers and polymer-based nanostructures

Polymeric nanocomposites have been found robust, cost-effective, highly efficient, and accurate for food hazard detection, which can combine with the ACQ effect. Conjugated polymers are very important members of the fluorescent material family because of their brilliant fluorescence properties and signal amplification potential (Wang, Zhang, et al., 2020). Conjugated polymer nanoparticles (CPNs) prepared from conjugated polymers not only remain the merits of conjugated polymers but also improve the defects of poor light stability and toxicity. Wang, Zhang et al. (2020) used CPNs with carboxyl groups as the active sites for detecting ascorbic acid with good linearity ($R^2 = 0.9903$) in the range of 0.57–17.10 μmol/L. Because of chelation and electrostatic interaction between CPNs and Fe^{3+}, the aggregates appeared, and fluorescence was quenched. However, ascorbic acid can reduce Fe^{3+} to Fe^{2+}, which disperses the aggregation of CPNs and Fe^{3+}, leading to fluorescence recovery (Figure 3c).

Semiconducting polymer nanoparticles, also named polymer dots (PDs), as a new class of fluorescent nanoprobes have also received extensive attention due to their excellent characteristics, such as tunable luminescence, high brightness, superior stability, and biocompatibility (Yuan et al., 2021). Nevertheless, PDs are generally hydrophobic and have a relatively large particle size, limiting their application in fluorescence sensors. Chabok et al. (2019) synthesized carboxyl-functionalized poly[(9,9-dioctylfluorenyl-2,7-diyl)-alt-co-(1,4-benzo-(2,1′,3)-thiadiazole)] (PFBT) PDs by a nano-precipitation technique to improve the water solubility. These PDs were applied in fluorescence sensors for Cu^{2+} or Fe^{3+} and the sandwich-like aggregation of PDs and Cu^{2+}/Fe^{3+} happened due to the interaction between the surface

carboxyl groups of PDs and Cu^{2+}/Fe^{3+} ions, leading to fluorescence quenching (Figure 3d). Furthermore, the addition of histamine would recover fluorescence because it could release the Cu^{2+} ions but it could not release the Fe^{3+} ions; thus, Cu^{2+} and Fe^{3+} ions could be distinguished.

Polymeric structure and reversible non-covalent interactions endow supramolecular polymers with high response to stimuli, environmental adaptation, and self-repairing capacity (Liu et al., 2021). However, weak bonding strength and poor stability of supramolecular polymers limit their application. Liu et al. (2021) designed and synthesized a new pillar[5]arene derivative P5-OXD to build fresh supramolecular brush polymers and develop fluorescent chemosensors with high selectivity toward Cu^{2+}. ACQ phenomenon was observed accompanied by a redshift during the formation of P5-OXD, and the fluorescence of the polymer went through further decrease in the presence of Cu^{2+}, indicating the possibility of changing into cross-linked supramolecular networks. The brush structure could enhance the coordination with targeted metal ions, leading to higher detection sensitivity.

The ACQ effect of polymers is mainly induced by metal ions through electrostatic interaction and electron or energy transfer. Attributed to the structural controllability, polymers possess high affinity with metal ions and facilitate in multiple solution environments.

2.2 | Aggregates with aggregation-induced emission effects

AIE effects are produced due to the restriction of intramolecular motion and inhibition of nonradiative decay. Aggregates with AIE effects can be categorized as carbon nanomaterials, MNCs, QDs, polymers and polymer-based nanostructures, organic molecules, and covalent organic framework (COF)/metal–organic framework (MOF) materials according to their molecular level compositions.

2.2.1 | Carbon nanomaterials

Apart from ACQ, many fluorescence sensors combined AIE effects with carbon nanomaterials such as CDs and GQDs with high fluorescence intensity. Li, Shi, et al. (2021) synthesized "turn-on" red fluorescent CDs as a sensor for tetracycline antibiotics detection in acidic addition (Figure 3e), and the aggregation was triggered by π–π stack interaction between CDs and tetracyclines. Because the rotation of functional groups on CD surface was restricted and the π-conjugated CDs were elevated under aggregation status, the fluorescence emission was enhanced. The analytes of this sensor included tetracycline, oxytetracycline, and chlortetracycline with detection limits of 12, 23, and 25 nmol/L. Gan et al. (2021) combined red emissive europium complexes (synthesized by adenine, dipicolinic acid, and Eu^{3+}) with blue emissive CDs (synthesized by citric acid and triethylenetetramine) to develop CD-based dual-emissive sensor (CDs@Ad–Eu–DPA), lowering the detection limit for Hg^{2+} to 0.2 nmol/L (Figure 3f). Through binding with the surface groups, Hg^{2+} induced the aggregation of CDs with increased blue fluorescence emission, whereas Hg^{2+} hindered the photoinduced electrons transfer process between adenine and dipicolinic acid of europium complexes, elevating red fluorescence intensity. Pathan et al. (2019) modified GQDs with Fe_3O_4 nanoparticles as magnetic nanoparticles (MNPs) (Fe-GQDs) to build up a fluorescence sensor for arsenic detection based on an AIE enhancement process (Figure 4a). The application of MNPs increased the number of binding sites, realizing the reusing of the material. Upon the addition of As^{3+}, Fe-GQDs and As^{3+} aggregated through multiple intermolecular interactions, leading to the increase of fluorescence emission with a redshift under the circumstances of all pH values.

Moreover, the ACQ and the AIE phenomena may coexist in fluorescence carbon nanomaterials, which have the potential for application in food hazard detection. Yang et al. (2019) prepared hydrophobic CDs, and their blue emissive carbonized cores went through ACQ under aggregation conditions, whereas the intramolecular motion of the surface symmetrical heterocycles about the disulfide bonds was limited, resulting in the red AIE effect (Figure 4b). Furthermore, Zhang, Zhuo et al. (2019) prepared a novel type of CD, in which the ACQ at a specific wavelength could be transformed into a fluorescence enhancement of AIE at another wavelength. A possible mechanism was that the residual blue emission energy of the dispersed CDs could be transmitted to the large yellow emissive aggregates of CDs due to FRET, and the blue light emitted by the dispersed CDs would be reabsorbed by the agglomerated CDs. Such CDs went through dual-emission change with obvious color change before/after aggregation, making them ideal candidates for ratiometric fluorescence sensor construction.

All in all, the aggregations of AIE-active carbon materials are commonly induced by π–π stack interaction or electrostatic interaction. In addition, the fluorescence intensity increases generally because the aggregation restricts the rotation of the functional group, elevates π-conjugate, and hinders the photoinduced electrons transfer process.

TABLE 2 Summary of ligands has been used for imparting the metal nanoclusters for the aggregation-induced emission (AIE) phenomenon.

Nanoclusters	Ligands	Functional groups of ligands	Reference
CuNCs	GSH	HS–, –COOH	Shen et al. (2019) and Zhao, Wang et al. (2022)
AuNCs	GSH	HS–, –COOH	Qu, Zhao et al. (2018) and Wei et al. (2023)
AuNCs	MUA/GSH	HS–	Lu et al. (2020)
AuNCs	6-Aza-2-thiothymine	HS–, $–NH_2$	Yue et al. (2022)
AgNC	Poly cytosine	$–NH_2$	Mortazavi Moghadam et al. (2021)
AgNC	Thiosalicylic acid	HS–, –COOH	Li, Xi et al. (2021)
AgNCs	Mercaptosuccinic acid	HS–, –COOH	Mahato et al. (2022)
AgNCs	2-Mercaptobenzothiazole	HS–	Packirisamy and Pandurangan (2021)
AgNCs	*N*-Acetyl-L-cysteine	HS–, –COOH	Sahu et al. (2019)
CuNCs	Silk fibroin	$–NH_2$, –OH	Ren et al. (2019)
CuNCs	L-2,3-Dihydroxybutanedioic acid	–COOH, –OH	Chen, Wang et al. (2021)
CuNCs	Melamine-formaldehyde microspheres	$–NH_2$, –OH	Li et al. (2022)
CuNCs	Phosphorus, nitrogen doped CDs, and GSH	$–NH_2$, –OH	Yin et al. (2022)

Abbreviations: AgNCs, Ag nanocluster; AuNCs, Au nanoclusters; CDs, carbon dots; CuNCs, Cu nanoclusters; GSH, L-glutathione; MUA, 11-mercaptoundecanoic acid.

2.2.2 | Metal nanoclusters

It has been acknowledged that metallic nanoclusters suffer from low quantum yields and photostability; many investigations have focused on the AIE effect of MNCs to increase the quantum yield but the improvement was often sophisticated and affected by many factors (Wei et al., 2023; Zhang, Zhao, et al., 2020). The AIE phenomenon of ligands-capped MNCs would be affected by the structure of ligands, and the types of ligands include acids (Ling et al., 2020; Lu et al., 2020), amines, thiols (Wang, Bai, et al., 2020), and proteins (Zhang, Zhao, et al., 2020), which are demonstrated in Table 2. Ligands that are anchored on individual well-dispersed Cu nanoclusters (CuNCs) can experience free movement, but those intramolecular motions will be restricted by the physical confinement due to aggregation, leading to the decrease of nonradiative recombination, and promotion of charge–transfer interaction between the metal cores and surface ligands, with corresponding fluorescence enhancement (Lu et al., 2020).

Glutathione (GSH) is a frequently used ligand of MNCs with latent AIE property. Shen et al. (2019) designed a novel Cu^{2+} sensing method using thiol-containing GSH as a reducing and stabilizing agent, whereas tetrahydrofuran (THF) as the poor solvent, according to the phenomenon that GSH rapidly reduced Cu^{2+} ions into a cluster, followed by a stable aggregation of the clusters in THF with a bright orange emission. The sensor exhibited linearities in the range of 0.25–10 μmol/L (R^2 = 0.998). Qu, Zhao et al. (2018) developed a dual-emissive sensor for Cd^{2+}, in which amino-modified SiNPs and GSH–AuNCs self-assembled into an aggregate through electrostatic interaction, exhibiting the unique AIE of GSH–AuNCs and the blue fluorescence of SiNPs. The addition of Cd^{2+} connected the nanospheres to form large aggregates, which further enhanced the AIE effect of GSH–AuNCs, whereas the emission of SiNPs remained unchanged as an internal reference (Figure 4c). The employment of emissive SiNPs elevated the sensitivity of the GSH–AuNCs-based Cd^{2+} sensor with a detection limit of 0.5 μmol/L.

Proteins and organic acids can also be applied as capped ligands for MNCs, some of which have been applied in sulfide detection. Aggregation of S–silk fibroin protein–CuNCs could be triggered by S^{2-}, leading to the AIE effect (Zhang, Wang, et al., 2019), whereas the aggregation of 11-mercaptoundecanoic acid–AuNCs could be induced by H_2S because the water solubility of AuNCs became lower in the existence of H_2S (Lu et al., 2020). Incorporating these two kinds of MNCs, the detection of sulfide in various pH environments may be achieved. Chen, Wang et al. (2021) synthesized a fluorescence sensor for Fe^{3+} based on micellar co-aggregation between green natural organic acid–capped CuNCs and novel deep eutectic solvent, as Fe^{3+} could quench the fluorescence emission of acid-CuNCs (Figure 4d). A relatively steady and enclosed microenvironment would form due to micellar co-aggregation, which prevented CuNCs from collisions with water molecules and elevated their fluorescence intensity.

In some cases, ACQ and AIE effects can be combined to build a high-sensitivity fluorescence sensor based on MNCs. Xu, Meng et al. (2018) reported green-emitting Au/Pt NCs capped with polyethyleneimine (PEI), which

could specifically detect chlortetracycline (Figure 4e). Upon the addition of different kinds of tetracycline antibiotics, Au/Pt NCs exhibited significant ACQ effects due to non-covalent interaction between tetracycline antibiotics and PEI. Meanwhile, a remarkable AIE effect was observed only in the presence of chlortetracycline after the further addition of Al^{3+}, because Al^{3+} could interact with chlortetracycline to form a hexatomic chelate ring, inhibiting the rotation of –OH and C=O and increasing the fluorescence.

The AIE effect of MNCs is usually because the analytes decrease solubility or bind with the surface group by some non-covalent interactions, promoting the charge–transfer interaction between the metal cores and surface ligands or activating the radiative decay. Recent studies tended to apply CuNCs in AIE sensor construction due to the advantages of low cost and hypotoxicity, but the stability required to be improved.

2.2.3 | Quantum dots

Despite the wide studies of the ACQ effect of QDs, many researchers focused on their AIE effects in food hazard detection, especially for metal ions. The introduction of the AIE phenomenon makes it easier to develop a "turn-on" sensor with outstanding detection limit (Cai et al., 2019). Kayal and Halder (2019) have applied an aromatic thiol, thiosalicylic acid (TSA), as a capped ligand to prepare ZnS QDs for soluble ppb-level total arsenic [As(III)+As(V)] detection in aqueous media, with low detection limits of 0.79 ± 0.01 ppb for As(III) and 2.79 ± 0.02 ppb for As(V). The binding between arsenic and the surface of ZnS QDs triggered the aggregation, enhancing the fluorescence emission of dispersed ZnS QDs (Figure 4f). Interestingly, this sensor was capable of distinguishing As(III) and As(V) because the addition of As(III) induced larger aggregates and higher fluorescence emission of QDs than As(V) at the same concentration. Zn–Ag–In–S (ZAIS) quaternary QDs rise in popularity owing to their facile synthesis, low toxicity, and high stability. Wei et al. (2019) synthesized aqueous ZAIS QDs, using L-cysteine as ligands to further decrease toxicity, for Cd^{2+} detection based on AIE enhancement (Figure 5a). Upon the addition of Cd^{2+}, leading to consequent aggregation and the formation of microheterojunctions between ZAIS QDs and the composite of Cd^{2+} and thiol anions (ZAIS/Cd-SR). As a result, non-radiative recombination was decreased, and the surface defect was passivated, ZAIS QDs exhibited higher fluorescence intensity.

AIE-active QDs usually exhibit the excellent fluorescent intensity and are alert to slight changes, making them qualified for the construction of super-selective sensors, which was capable of distinguishing metal ions with different valences.

2.2.4 | Organic molecules

Many organic molecules with the AIE effect have been synthesized because it is relatively easy to manipulate their structures in order to make their emission property suitable for practical applications (Hong et al., 2011). Among the AIE-active molecules that have been applied in fluorescence sensors, tetraphenylethylene (TPE) and its derivatives receive wide attention (Hong et al., 2011). This is because the absorption and emission properties of the functionalization of TPE can vary upon the binding of guests (anions and cations) in either polar or nonpolar solvents (Hu, Qin, et al., 2020). TPEDB, being obtained by functionalizing TPE with two boronic acid units, can form a cross-linked network with glycoclusters to exhibit the AIE effect (Figure 5b). As the formation of the network is reversible, Li et al. (2020) designed a method for phenols pollutant detection because phenols could destroy the network, release TPEDB, and quench the fluorescence. Combining TPEDB with a new NIR-emissive AIEgen DCQA, a dual-AIEgen system without spectral overlap has been designed and fabricated for microbial viability quantification and biofilm formation monitoring (He et al., 2021). DCQA possesses the ability to stain all kinds of microbes, but TPEDB is only capable of recognizing specific dead. The application of this dual-AIEgen system realized the in situ quantitation of microbial viability and supervision of biofilm formation, indicating great prospects in foodborne pathogen supervision. Selvaraj et al. (2021) fabricated a novel AIE luminophore via conjugating TPE with bis(thiophen-2-ylmethyl)amine (BTA) for highly selective and sensitive Hg^{2+} detection because the binding between Hg^{2+} and BTA promoted the aggregation of luminophores and increased the fluorescence intensity, and the TPE–BTA fluorescent probe exhibited a low detection limit of 10.5 nM and a 1000-fold selectivity compared with other metal ions.

Besides TPE, other AIE-active molecules are also available. 2-(20-Aminophenyl)benzothiazole (APBT) has been known as an excited-state intramolecular proton transfer (ESIPT) active compound; especially, its amide derivative can facilitate the ESIPT event and lead to a long wavelength emission. Tang, Xia et al. (2020) synthesized a simple APBT-derived BTPPA with AIE property as a Cu^{2+} sensor with high sensitivity and a good linear correlation ($R^2 = 0.997$). The aggregates of BTPPA would be destroyed by Cu^{2+} through BTPPA–Cu^{2+} binding, leading to fluorescence quenching. Wang et al. (2021) developed a tripodal acylhydrazone derivative, which could self-assemble into

an organogel with a bluish–green AIE effect. Al^{3+} could be sensed with a detection limit of 8.702×10^{-7} mol/L when it was added to the system because it would coordinate with organogel to form larger complexes, leading to emission change from bluish–green to green.

Generally, electrostatic interaction, hydrogen bonds, reversible covalent bonds, and poor solubility would cause AIE-active molecules aggregates, leading to the restriction of intramolecular motion with the fluorescence emission. In order to increase the sensitivity, researchers focused on introducing NIR AIE-active molecules in AIE-based organic molecules sensors.

2.2.5 | Polymers and polymer-based nanostructures

AIE polymers integrate the advantages of luminescent polymeric materials and AIEgens, showing unique properties, such as good solubility, operability, and emission efficiency in the aggregated states (Hu, Qin, et al., 2020). However, AIE polymers still meet with some challenges, such as their short-wavelength absorption, a broad emission spectrum, and safety issues, limiting their usage in practical food hazard detection (Chowdhury et al., 2022). With the integration of the AIE-active molecules into polymer chains, the free rotation of the embedded luminogenic units exposed inherently steric hindrance of the long-chain segments of polymers, exhibiting higher fluorescence emission. Generally, typical AIE-active molecules, including TPE, distryre-neathracence (DSA), hexaphenylsilole (HPS), 1,8-naphthalimide,2,4,6-triphenylpyridine and tetraphenylpyrazine (TPP), and (2-(4-vinylphenyl)ethene-1,1,2-triyl) tribenzene (TPEE), are widely utilized to prepare AIE polymers (Hu, Qin, et al., 2020). The polymer chains can be used as substrates for AIE-active molecules, including amphiphilic polymers, conjugated polymers, block copolymers, and polysaccharides. The integration of AIEgens with nanoparticles composed of amphiphilic polymer building blocks has drawn significant attention due to the advantages of emission brightness, fluorescence stability, and excellent water solubility. Zhou et al. (2019) modified amphiphilic polymer with TPE to form self-assembly micelles named AIE dots, providing water dispersibility and bio-functionality for AIE-active molecules (Figure 5d), and showed that the hydrophobic polymers and TPE moiety organized into the core with AIE effects due to rotational constraints, and the water-soluble polymers acted as the corona. Organic amines could be detected because they were captured by the water-soluble polymers and transported into the core due to hydrophobic and $\boldsymbol{\pi}$–$\boldsymbol{\pi}$ interaction, causing fluorescence quenching of TPE. The water-soluble corona endowed the micelles with superior dispersibility in water and produced an amplification effect through amine enrichment, leading to high sensitivity and rapid response. However, AIEgens amphiphilic polymeric nanoparticles are usually short-wavelength absorption and non-biodegradable, limiting the application in food detection. Liposomes are amphiphilic, biocompatible, and biodegradable materials, which show potential as multifunctional nano-carriers of AIEgens. Shen, Wei, Chen et al. (2022) and Shen, Wei, Zhu et al. (2022) constructed liposome-encapsulated AIEgens for achieving the visual on-site detection of residual tetracycline. TPE was encapsulated into an amphiphilic phospholipid polymer to develop AIEgen liposome, whereas Eu^{3+} could bind with the negative charge phospholipid on the surface of AIEgen liposome. As the new red fluorescence emission would emit when Eu^{3+} chelated with tetracycline, especially in assistance with citrate, a remarkable dual emission sensor for a ratiometric tetracycline detection was built up with a low detection limit of 28.83 nmol/L.

Conjugated microporous polymers (CMPs) are a class of amorphous structures that have recently attracted increasing attention in chemical sensing due to their extended π-conjugated framework, permanent microporous structure, and large specific surface area (Liu, Wang, et al., 2020). However, structural rigidity derived from CMPs' stable π-conjugated skeleton results in insolubility and poor processability, which requires improvement in further studies (Zhang, Zuo, et al., 2022). Liu, Wang et al. (2020) designed an AIE-active CMP, with TPE acting as core and carbazole group acting as electro-active branches, to determine volatile organic compounds (VOCs), which has the potential for applying in food safety hazards detection. 2D sensing array is established through CMP films and their monomer spin-coated films, and 18 types of VOC vapors have been precisely distinguished by linear discriminant analysis. VOCs could be sensed because they diffused into the microporous structure and limited the free rotation of TPE groups, leading to the AIE effect (Figure 5c). The microporous structure was beneficial to the diffusion of VOC vapors into the films, which contributed to the high sensitivity for VOC detection.

Advanced polymers could encapsulate or bind to AIE-active molecules to aggregate the molecules and induce the AIE effect. Due to the advantages of operability and emission efficiency, AIE polymers were favorable materials in sensor construction.

2.2.6 | Covalent organic frameworks/metal–organic framework materials

COFs are a class of extended crystalline organic materials that possess unique architectures, such as high surface area and tunable pore sizes formed by the covalent linkages of organic building blocks (Dong et al., 2018). Tang, Huang et al. (2020) developed luminescent porous materials for simultaneous detection and removal of the nitrofurans in water by constructing AIE-active molecules 4′,4‴,4⁗,4⁗′-(ethene-1,1,2,2-tetrayl)tetrakis(([1,1′-biphenyl]-4-carbaldehyde)) (ETTC) monomer into 2D porous covalent triazine framework nanosheets followed by a change in the electron transition energy and an increase in the luminous efficiency. Nitrofuran detection was realized based on the emission quenching due to energy and electron transfer between covalent triazine framework nanosheets and analytes, and the detection sensitivity was enhanced because the fluorescence quenching efficiency was improved by the absorption-induced preconcentration effect of 2D porous covalent triazine frameworks. However, in many cases, frameworks possessed inferior crystallinity and porosity, which limited the sensitivity when COF was applied in chemosensors.

Compared with COFs, MOFs possess higher crystallinity, which are crystalline hybrid coordination polymers consisting of ions/clusters as nodes and organic ligands as linkers (Zhang, Huang, Sun, & Pu, 2022; Sun, Huang, Pu, & Ma, 2021). Due to the inherent properties of simple synthesis, microporosity, high loading capacity, and confinement effect, MOFs become preferable materials to construct AIE-based sensors. However, the strength of the coordination bond in MOFs is usually not strong enough, restricting their applications under harsh conditions (Huang, Sun, & Pu, 2022; Xie et al., 2020). Gao et al. (2020) encapsulated GSH–CuNCs and Al^{3+} mixtures into a zeolitic imidazole framework (ZIF)-90 to build a fluorescence sensor with high adenosine triphosphate (ATP) sensitivity in aquatic products (detection limit of 0.67 μmol/L). Due to the ability of ATP to cause the collapse of ZIF-90 and to break the coordination between CuNCs and Al^{3+}, in the presence of ATP, CuNCs would release from the MOFs with the occurrence of fluorescence quenching (Figure 5g). The sensor was sensitive because of the high fluorescence efficiency of GSH–CuNCs and Al^{3+} complexes, as their vibrations were suppressed by the rigid ZIF-90. However, other researchers reported that the emission of the encapsulated luminescent species might be limited and trapped in the MOFs, to counteract this problem, Xie et al. (2020) synthesized a series of novel luminescent MOFs as Cu^{2+} sensors by binding AIEgens ((e)-2-((2-aminophenylimino)methyl)phenol) on the surface of nanoscale ZIF-8, allowing good dispersion of the MOFs in solutions. The fluorescence intensity of AIEgens exhibited significant elevation because their rotation was confined, and emission was induced on the surface of the ZIF-8 frame, offsetting the negative influence of MOFs on the AIE phenomenon. The detection procedures were based on the fluorescence quenching due to electrons or energy transfer from MOF to Cu^{2+}. Part of the MOFs themselves possessed the AIE property, which was induced by the addition of detection analytes. Zhang, Ren et al. (2020) fabricated a 2D luminescent Cd(II)-organic framework as a "turn-on" Fe^{3+} sensor because the framework and Fe^{3+} would form a sandwich-like arrangement with the $\boldsymbol{\pi}$–cation–$\boldsymbol{\pi}$ packing model, promoting the electron transfer efficiency within the framework, elevating the emission intensity.

In addition, the highly sensitive sensor could be achieved when Yin et al. (2019) combined Ln^{3+} ions with AIEgens to develop an MOF-based dual-emission fluorescence sensor. The sensor was designed using MOFs with an AIE ligand (1,4-terephthalic acid) and Ln^{3+} ions (including Eu^{3+}, Tb^{3+}, and Gd^{3+}) (Figure 5f), in which the triple-state sensitized Ln^{3+} ions exhibited stable bright red emission due to the antenna effect (Eu^{3+} ions exhibited the strongest emission), and the AIE ligands exhibited blue emission because of their restricted intramolecular rotation. After the addition of arginine as the analyte, the conjugate range was expanded, and the blue emission was enhanced, whereas the red emission remained unchanged, thus acting as a reference for ratiometric fluorescence sensing and visible detection. This sensor also has the potential of being used in food hazard detection.

Both COFs and MOFs exhibit development potential in AIE-based sensors, due to their high surface area and tunable pore sizes. Especially for MOFs, not only it can be applied to immobilized AIEgens on their surface or in their micropores to induce the AIE effect with high stability but also can be used as AIE-active fluorescent materials to provide fluorescence signal in contact with target analytes.

3 | SENSING COMBINED WITH RECOGNITION UNITS

In order to improve the selectivity and sensitivity of aggregate-based sensors, recognition units can be applied with ingenious strategies. Commonly used units include aptamer, antibody, molecular imprinting, and host–guest recognitions.

3.1 | Aptamer

Aptamers are single-stranded oligonucleotides that can selectively bind to target molecules, which are stable, programmable, and suitable for site-specific labeling. Their versatility boosts the development of aggregate-based aptasensors in food hazard detection because the participation of aptamers widens the range of analytes (Zhao, Kong, et al., 2019). Esmaelpourfarkhani et al. (2020) deposited aptamers on the surface of AuNPs, hybridized them with their complementary DNA (cDNA), and combined them with a low-cost fluorophore (3,4,9,10-perylenetetracarboxylic acid diimide (PTCDI)), to develop an ACQ aptasensor for selective ampicillin detection with a linear fit in the range of 100–1000 pmol/L ($R^2 = 0.9942$) (Figure 6a). Upon its addition, the ampicillin bound to aptamers and released the cDNA, which could be separated by centrifugation and finally existed in the supernatant. The quantity of isolated cDNA can be detected by means of triggering the ACQ of PTCDI. This process is initiated when the nucleic acid sequence interacts with the fluorophore via π–π interaction and hydrogen bonding. Terminal deoxynucleotidyl transferase–catalyzed DNA polymerization could be applied to elongate DNA and further enhance its sensitivity (Wang, Zheng, et al., 2019). Li, Guo et al. (2019) developed a label-free, simple, and sensitive AIE aptasensor for ATP detection, using 9,10-distyrylanthracene derivative with short alkyl chain (DSAI) as an AIEgen (Figure 6b). This sensor also has the potential of being used in monitoring food freshness. In the sensing system, the presence of ATP would combine with aptamer and change the conformation of the aptamer to prevent it from digestion by Exo. I. After the addition of DSAI, the DSAI would aggregate on the surface of the aptamer/ATP complex due to the electrostatic interactions between the ammonium cation in DSAI and backbone phosphate anions in aptamers and the hydrophobic interaction between aryl rings in DSAI and nucleosides in aptamers, leading to the AIE phenomenon. Zhao, Kong et al. (2019) modified aflatoxin B_1 (AFB_1) aptamer with tetramethylrhodamine (TAMRA) fluorophore at the terminal in order to create an intrinsic conformation response-leveraged aptamer probe for detecting AFB_1 with high sensitivity (detection limit of 0.29 ng/mL), similarly using the AIEgen DSAI (Figure 6c). AFB_1 would combine with aptamer and change the intrinsic conformation, which reduced the AIE effect of DSAI due to the disruption of the double-stranded structure but increased the FRET effect from DSAI to TAMRA fluorophore due to closer proximity. The participation of the FRET process improved the sensitivity of AIE-based AFB_1 aptasensor because the dual-wavelength variation response to target molecules would combinedly amplify the output signals. Jia, Wu et al. (2019) employed graphene oxide (GO) as a fluorescence quencher to design a new AIE-based AFB_1 aptasensor (Figure 6d). Due to electrostatic interaction, the negatively charged DNA backbone could spontaneously induce the AIE effect of positively charged quaternized TPE. The AIE phenomenon of the quaternized TPE and aptamer complexes was quenched by GO, which would recover in the presence of AFB_1 because it could release the complexes from GO through binding with AFB_1 aptamer. The introduction of GO and TPE-Z endowed the sensor with low background fluorescence signal and photostability, favoring the detection of AFB_1.

Aptamers participate in aggregation in multiple ways, making them useful in aggregate-based sensors. First, their cDNA would aggregate the fluorophore by electrostatic interactions. Second, the aptamer can act as an aggregation preventer, but this function would vanish when their conformation change. Third, analytes shorten the distance of fluorophores modified at the terminals of aptamers through conformational changes, leading to the change of the AIE effect or FRET process. Encouraged by past success, more researchers have joined the force of aptamer selection in the construction of aggregate-based sensors. However, Zhao, Yavari et al. (2022) concluded that it was a challenge to distinguish between non-aptamer sequences and true aptamers during aptamer selection. Without appropriate controls, non-aptamer sequences might show false positive binding results. Sensors designed using these sequences would then not produce reliable analytical results. Therefore, the binding ability of some aptamers requires careful evaluation in future studies.

3.2 | Antibody

Antibodies are the most popular bioreceptors to design various types of biosensors due to their high affinity and specific binding, exhibiting higher accuracy compared with aptamer but still remaining some defects, such as poor solubility and low thermal stability. AIE phenomenon has been applied in immunochromatographic assays, fluorescence-linked immunosorbent assays (FLISA), and enzyme-linked immunosorbent assays (ELISA) to significantly improve detection sensitivity. Wang, Hu et al. (2019) used AIE fluorescent microsphere (FM) as the replacement of colloidal gold to construct a novel competitive lateral flow immunoassay for sulfamethazine with a limit of detection (LOD) of 0.028 ng/mL, which was at least five times lower than using other fluorescent dyes. Wu et al. (2020) designed a novel AIE-based FLISA platform by constructing AIEgens nanobeads coupled with antibodies for sensing through sandwich format, improving the sensitivity by up to 12-fold compared with FLISA using

commercial green QD nanobeads as the label. AIEgens were first functionalized by conjugating streptavidin, followed by coupling with a biotinylated detection antibody. AIE effect can be regarded as an outstanding signal for the existence of labeling enzymes in ELISA, in particular, alkaline phosphatase (ALP) can be applied as a labeling enzyme to catalyze the hydrolysis of ascorbic acid–phosphate to generate ascorbic acid, leading to the reduction of Cu^{2+} into Cu^{+}. Li, Liu et al. (2019) introduced a DNA template to construct a fluorescence signal for ALP in the ELISA platform; due to the resultant ascorbic acid, Cu^{2+} and DNA templates would be in situ synthesized by click reaction, and the DNA-templated CuNCs displayed the AIE phenomenon. Yu et al. (2019) noticed the problem that the complexity of click reaction might burden practical applications of current ELISA platforms and designed a novel AIE-based ELISA, which could be directly applied to the current immunoassay platforms, offering a 2.5-fold increase in sensitivity compared with conventional ELISAs (Figure 6e). The glucose oxidase was applied as a labeling enzyme to catalyze the oxidation of glucose for H_2O_2 production, and H_2O_2 was capable of stimulating the aggregation of TPE derivative with fluorescence emission.

Guo et al. (2020) fabricated immunoglobulin G (IgG)–TPE–OH@BSA NPs via encapsulating TPE–OH in bovine serum albumin (BSA) microspheres and labeling rabbit IgG antibodies on its surface followed by combining them with aptamer–MNPs to specifically capture *Listeria monocytogenes* (Figure 7a). Due to the AIE effect in BSA, TPE–OH endowed the nanoparticles with the fluorescence emission. In the presence of *L. monocytogenes*, aptamer–MNPs and IgG–TPE–OH@BSA NPs self-assembled and then formed into a sandwich-type immune complex, which could be easily deposited by an external magnetic field for further fluorescence measurements.

In aggregate-based sensors combined with immunoassay, the recognition process and aggregation process are usually separated. As for the aggregation process, AIEgens have already aggregated as excellent fluorescent labels in lateral flow immunoassay and FLISA, whereas their aggregation is initiated by enzyme-coupled antibodies in ELISA.

3.3 | Molecular imprinting

Molecularly imprinted polymers (MIPs) are synthetic polymeric materials possessing specific binding cavities with shape and functional groups complementary to the target molecule. MIPs have desirable features as receptors, such as high chemical stability, ease of processing, and excellent functionality under harsh conditions, but their specificity and affinity are generally considered to be lower compared with natural enzymes or antibodies (BelBruno, 2019). Li, He et al. (2019) combined vinyl group functionalized TPP AIEgens with MIP by precipitation polymerization to develop a ratiometric fluorescence sensor for rhodamine 6G in food with a linear fit in the range of 0.0–10.0 μmol/L (R^2 = 0.997). The application of MIP endowed the sensor with fast mass transfer and high site accessibility for analytes, contributing to the high detection efficiency (Figure 7c). Upon the recognition of rhodamine 6G, a part of excitation light for AIE-MIPs was adsorbed by rhodamine 6G and the original fluorescence intensity from AIEgens declined, whereas the new fluorescence emission peak gradually elevated, indicating a ratiometric fluorescence change that could be perceived by naked eyes. Similarly, after combining acrylic group–modified TPE with MIPs, rhodamine B can also be detected through the same strategy (Li, Hou, et al., 2019). Tan et al. (2019) designed a spherical MIP for metronidazole detection in an aqueous solution, in which GSH–AuNCs, as the signal part due to their AIE properties, were anchored on the surface of silica-protected Fe_3O_4NPs (Figure 7d). After the enrichment of metronidazole under an external magnetic field by this MIP, the occurrence of charge transfer from the GSH–AuNCs to analytes resulted in fluorescence quenching. As an extension of MIPs, bacteria-imprinted polymers (*N*-Succinyl-Chitosan doping bacteria-imprinted composite film) with enjoyable bacterial identification ability have been applied in the AIE sensor for *Staphylococcus aureus* as a facile strategy with LOD as low as 6.9 CFU/mL (Guo et al., 2022). After imprinted film captured *S. aureus*, it would react with AIE-active AuNPs due to electrostatic interaction, leading to a decrease in the amount of AuNPs and fluorescence intensity in the supernatant.

Most AIEgens would immobilize on MIPs to exhibit their AIE effect, and the sensitive detection is realized through the analytes enrichment and AIE fluorescence quenching. But so far, the sensors are generally "turn off" type, limiting the practical application because false positive results will happen in those sensors.

3.4 | Host–guest recognitions

In many cases, supramolecular assemblies can be developed by synthesizing a concave "host" molecule that contains a recognition motif for a specific secondary "guest" molecule. The specific host–guest recognition demonstrates a great potential for participation in aggregate-based fluorescence sensors due to its ultrahigh affinities toward the target analytes and multi-tunable photophysical properties. However, host–guest chemistry still cannot

be fully understood in water, and the recognition will be interrupted by different nutrients (Beatty & Hof, 2021). Song et al. (2019) combined AgNPs with the carbonyl portals of cucurbit[6]uril (CB[6]) through electrostatic interactions to synthesize CB[6]-AgNPs as a naked-eye probe of metformin (MET). Based on the host–guest molecular recognition, the guanidine group of MET could be incorporated into the cavity of CB[6], leading to the aggregation of CB[6]-AgNPs with a color change from light yellow to light red (Figure 7e); visual identification associated with UV–Vis spectral analysis for MET was developed for the first time. Jia, Xu et al. (2019) employed multiple anchored fluorene dimers (8Py-2F) to develop a highly sensitive aggregate-based sensor because the aggregation of the 8Py-2F could be triggered by dinitrate through host–guest recognition as the fluorescence change (Figure 7f). After adding different amounts of dinitrate, aggregates of 8Py-2F in different sizes appeared, and the fluorescence of fluorene dimer was quenched to different extents with diverse color changes, making the sensor suitable for quantitative analysis. Using para-sulfonatocalix[4]arene (pSC4) capped gold nanoparticles (pSC4-AuNPs), Niu et al. (2022) presented a label-free sulfamethazine colorimetric sensor with high sensitivity as a correlation coefficient of 0.9908, ranging from 2.5 to 20 nmol/L. Sulfamethazine could bind to pSC4-AuNPs through host–guest recognition between its -NH_2 and sulfonamide groups and the macrocyclic cavity of pSC4, leading to the aggregation of pSC4-AuNPs, which can be observed through colorimetric assay.

Xu, Chen et al. (2018) fabricated a supramolecular network with two emission bands, containing coumarin with ACQ properties and TPE with AIE properties, to construct multiple ratiometric fluorescent sensors (Figure 7g). The supramolecular polymer network was formed upon Zn $(OTf)_2$ addition through metal-coordination and host–guest interactions, enhancing the fluorescence of the TPE and decreasing the fluorescence of the coumarin. The network showed ratiometric fluorescent sensing toward Cl^-, Et_3N, and cyclen due to the stimuli-responsiveness of the two non-covalent interactions.

Besides, host–guest recognition can also be used to destroy aggregates, offering another strategy to develop sensing systems. Through rationally introducing guest competitive controlled AIE into a trisnaphthalimide derivative-based supramolecular sensor, Lin et al. (2019) synthesized the selective and sensitive sensor of picric acid (PA) and CN^- (Figure 7b). The supramolecules self-assembled through hydrogen bonding and $\boldsymbol{\pi}$–$\boldsymbol{\pi}$ interaction of amido-modified trisnaphthalimide, leading to AIE phenomenon. The PA would destroy the assemblies and form TG–PA complexes through host–guest recognition, whereas CN^- could break the hydrogen bonding between TG and PA and recover the fluorescence of the TG assemblies.

Generally, host–guest recognition can be the motive power of the aggregation or dispersion, accompanied by fluorescence change. Through ingeniously introducing host–guest recognition in aggregate-based sensors, multicomponent detection can be realized.

4 | APPLICATIONS IN FOOD HAZARD DETECTION

Food hazards can be biological (such as mycotoxins and pathogens), chemical (such as food additives, pesticides, veterinary drugs, and metal cations), and physical contaminants (such as extraneous dirt), which can occur at production, packaging, transportation, and storage stages (Zhang, Ma, & Sun, 2020; Esua, Cheng, & Sun, 2020; Lu, Ma, & Sun, 2022). For sensitive and accurate detection, aggregate-based fluorescence sensors have been widely studied in detecting these hazards. Table 3 summarizes the applications of aggregate-based fluorescence sensors in food hazard detection.

4.1 | Food additives

Both overused and misused food additives will cause serious damage to human and animal health, making them one kind of food hazard (Li, He, et al., 2019). Thus, the detection of illegal usage of food additives becomes important and requires techniques with high sensitivity and rapidity.

Sulfides like sodium sulfide and hydrogen sulfide are widely used in agriculture and food industries as preservatives and flavor enhancers due to their antioxidant and antiseptic properties (Huang et al., 2021). High levels of sulfide can cause serious health problems, making it crucial to have a sensitive and efficient S^{2-} detection method for detecting sulfur-containing substances to ensure food safety. Wang, Bai et al. (2020) and Wang, Zhang et al. (2020) developed a sensor based on 3-mercaptopropionic acid functionalized CuNCs with AIE effect to detect S^{2-} in food additives as the fluorescence of 3-mercaptopropionic acid-CuNCs would be quenched by S^{2-}, and this sensor performed linearly in the range 0–600 μmol/L. The recoveries of three different spiked concentrations of S^{2-} ranged from 95.30% to 105.1%, which indicated the accuracy of the sensing platform. Melamine is an organic compound with a triazine heterocyclic structure that is typically found in low levels in food. However, due to its low cost and high nitrogen content, it can be illegally added to milk to increase protein levels, causing serious

TABLE 3 Summary of applications of aggregate-based fluorescence sensors in food hazard detection.

Analyte	Fluorescence materials	Mechanism	Linear range and LOD	Reference
Rhodamine 6G	Tetraphenylpyrazine-based polymer	AIE, MIP	0.0–10.0, 0.26 μmol/L	Li et al. (2020)
Rhodamine B	TPE-based polymer	MIP, Rhodamine B quench the AIE	0.0–10.0, 1.41 μmol/L	Li, Hou et al. (2019)
Melamine	Au@ CQD nanocomposites	AuNPs aggregate avoiding FRET to CDs	1–10 μmol/L, 3.6 nmol/L	Hu et al. (2019)
Melamine	6-Aza-2-thiothymine-AuNCs	AIE, fluorescence lateral flow assay	0.5–200 μmol/L, 45 nmol/L	Yue et al. (2022)
Sulfide ions	3-Mercaptopropionic acid-functionalized CuNCs	AIE of CuNCs, S^{2-} destroying aggregate, leading to quench	0–600 μmol/L, 26.3 nmol/L	Wang, Bai et al. (2020) and Wang, Zhang et al. (2020)
Terbuthylazine and dimethoate	Citrate-stabilized AuNPs	AIE	TBA(0.1–0.9 μmol/L), DMT (1–40 nmol/L)	Chen et al. (2018)
Atrazine	Nitrogen-doped CQDs	AIE	5 pmol/L–7 nmol/L, 3 pmol/L	Mohapatra et al. (2018)
Thiram	GSH–AuNCs	AIEE	0.05 μg/mL	Zhao, Kong et al. (2019) and Zhao, Yang et al. (2019)
Phoxim	CDs–AgNPs	Aggregate changing emission	0.1–100, 0.04 μmol/L	Zheng et al. (2019)
Paraoxon	Au NCs	AIE	3.3×10^{-14} mol/L	Liang and Han (2020)
Methyl parathion	CuNCs anchored on melamine–formaldehyde microspheres	AIE	0–6, 0.04 ppm	Li et al. (2022)
Chlorpyrifos	DNA–AuNCs	ACQ	0–80.0, 0.50 μmol/L	Lu et al. (2018)
Chlorpyrifos	Tb–MOFs and PDDA–AuNPs	Aptamer recognition, aggregate preventing FRET	5–600 nmol/L, 3.8 nmol/L	Liu et al. (2019)
Chlorpyrifos	GQD-capped gold nanocomposite	AIE	0.001–1.0 μg/mL, 0.0007 μg/mL	Chungchai et al. (2019)
Acetamiprid	Apt–CQDs	Aptamer recognition, ACQ	0.2–20, 0.04 ng/L	Jiao et al. (2018)
Acetamiprid	Apt-cCDs synthesized from cetrimonium bromide	Aptamer recognition, ACQ	1.6–120, 0.3 nmol/L	Saberi et al. (2019)
Sulfamethazine	*Para*-Sulfonatocalix[4]arene-AuNPs	AIE, MIP	1.39, 2.5–20 nmol/L	Niu et al. (2022)
Sulfamethazine	AIE fluorescent microsphere	Immunoassay, AIE	0.05–5, 0.028 ng/mL	Wang, Zheng et al. (2019) and Wang, Hu et al. (2019)
TC	Red fluorescent CDs	AIEE of CDs upon TC	3–35, 2–50, and 5–50 μmol/L, 12, 23, and 25 nmol/L	Jia, Li, Chen et al. (2021), Li, Wang et al. (2021), Li, Shi et al. (2021), and Li, Xi, et al. (2021)

(Continues)

TABLE 3 (Continued)

Analyte	Fluorescence materials	Mechanism	Linear range and LOD	Reference
TC	Eu^{3+}-functionalized liposome-based TPE	AIE	0.0961–10.0 μmol/L	Shen, Wei, Chen et al. (2022) and Shen, Wei, Zhu et al. (2022)
CTC	Polyethyleneimine-capped bimetallic Au/Pt NCs	ACQ	0.5–10, 0.35 μmol/L	Xu, Chen et al. (2018) and Xu, Meng et al. (2018)
CTC	DSA derivative, GO	Aptamer recognition, AIE	1.26 pg/mL	Zhang et al. (2018)
CTC	Zn–BTEC	CTC aggregate in rigid MOFs, AIEE	0–8 μmol/L, 28 nmol/L	Yu et al. (2019)
Ampicillin	Fluorescence dye, AuNPs	Aptamer recognition, ACQ	100–1000, 29.2 pmol/L	Esmaelpourfarkhani et al. (2020)
Amoxicillin	Tris–HCl buffer, AuNPs	Aptamer recognition, AIE	0.1–125 nmol/L, 67 pmol/L	Nguyen et al. (2022)
Metronidazole	GSH–AuNCs	MIPs, AIE	0–5 μmol/L, 4.2 nmol/L	Tan et al. (2019)
Amantadine	TPE	Immunoassay, AIE	0.38 ng/mL in buffer, 0.06 μg/kg in chicken samples	Yu et al. (2019)
Fumonisin B_1	AuNP	AuNP aggregation	3.125–25, 12.5 ng/mL	Chen et al. (2018)
AFB_1	TPE-Z, GO	AIE, aptamer	0–3, 0.25 ng/mL	Jia, Xu et al. (2019) and Jia, Wu et al. (2019)
Ochratoxin A	DSAI, Exo. I	AIE, aptamer, Exo. I degradation	5–500, 1.9 ng/mL	Lv et al. (2019)
AFB_1	PAPDI, AuNPs	ACQ, aptamer, DNA polymerization	0.05–50.0, 0.01 nmol/L (3.1 pg/mL)	Wang, Bai et al. (2020) and Wang, Zhang et al. (2020)
Patulin toxin	TTAPE dye	AIE, aptamer, strand displacement amplification	0.001–100 ng/mL, 0.042 pg/mL	Zhang, Duan et al. (2020)
AFB_1	DSAI, Exo. I	AIE, aptamer, FRET	0.29 ng/mL	Zhao, Kong et al. (2019) and Zhao, Yang et al. (2019)
Ochratoxin A	DSAI, Exo. I	AIE, aptamer, Exo. I degradation	0.5–30, 0.4 ng/mL	Zhu et al. (2019)
Staphylococcus aureus or *Escherichia coli*	TPE derivative	electrostatic reaction	10^6 CFU/mL	Chen et al. (2018)
E. coli	Glucose-based acrylamides	AIE, protein recognition	*E. coli* 7.30×10^5 cells/mL	Ajish et al. (2018)
Listeria monocytogenes	TPE-OH	AIE, aptamer, antibody	10–10^6, 10 CFU/mL	Guo et al. (2020)
E. coli O157:H7	TCBPE	AIE, immunochromatographic assay	3.98×10^3 CFU/mL	Zhang, Zhuo et al. (2019)

(Continues)

TABLE 3 (Continued)

Analyte	Fluorescence materials	Mechanism	Linear range and LOD	Reference
Cu^{2+}	APTEs–ZnO QDs	ACQ	1.72 nmol/L	Zou et al. (2020)
Hg^{2+}, Cu^{2+}, Fe^{3+}	Supramolecular polymer gels	AIE	10^{-11} mol/L	Chen et al. (2019)
Total As	Thiosalicylic acid–capped ZnS–QDs	AIEE	As(III) (0.79 ± 0.01 ppb), As(V) (2.79 ± 0.02 ppb)	Kayal and Halder (2019)
Lead	CuNCs–CNQDs	AIEE	0.010–2.5, 0.0031 mg/L	Li et al. (2020)
Lead	AgNCs	AIE	5–50, 3.0 nmol/L	Zhang et al. (2018)
Cr^{3+}	AgNCs	AIE	2–40, 0.71 μmol/L	Ren et al. (2019)
Hg(II)	CuNC	AIE	1–500, 0.3 nmol/L	Wang, Bai et al. (2020) and Wang, Zhang et al. (2020)
Cd^{2+}	ZAIS QDs	AIEE	25 umol/L–2 mmol/L, 1.56 umol/L	Wei et al. (2019)
Hg^{2+}	PMDP-G	AIE	7.3×10^{-10}–9.5×10^{-9} mol/L	Zhang, Zhuo et al. (2019)
CN^-	Bi-acylhydrazone supramolecular gelator	AIE	0.50 nmol/L	Qu et al. (2021)
Fluoride	$CH_3NH_3PbBr_3$ PQDs	ACQ	3.2 μmol/L	Liu et al. (2018)
Aliphatic amines	Amphiphilic triblock copolymer	AIE	8 μg/L	Zhou et al. (2019)
$K_4[Fe(CN)_6]$	SiQDs	ACQ	0.05–8.0 μg/mL, 30 ng/mL	Na et al. (2019)

Abbreviations: ACQ, aggregation-caused quenching; AFB_1, aflatoxin B_1; AgNCs, Ag nanocluster; AIE, aggregation-induced emission; AIEE, aggregation-induced emission enhancement; Apt, aptamer; APTEs-ZnO QDs, (3-aminopropyl) triethoxysilane coated zinc oxide quantum dots; AuNCs, Au nanoclusters; AuNPs, Au nanoparticles; cCDs, cationic carbon dots; CDs, carbon dots; CQDs, carbon quantum dots; CTC, chlortetracycline; CuNCs, Cu nanoclusters; CuNCs-CNQDs, Cu nanoclusters @ nitrogen-doped carbon quantum dots; DMT, dimethoate; DSA, 9,10-distyrylanthracene; DSAI, 9,10-distyrylanthracene derivative with short alkyl chain; FRET, fluorescence resonance energy transfer; GO, graphene oxide; GQDs, graphene quantum dots; GSH, glutathione; LOD, limit of detection; MIP, molecularly imprinted polymer; MOF, metal-organic framework; PAPDI, *N*,*N*′-bis(propylenetrimethylammonium)-3,4,9,10-perylenediimide; PDDA, poly-dimethyl diallyl ammonium chloride; PMDP-G, pillar[5]arene based supramolecular polymer; QDs, quantum dots; TBA, terbuthylazine; TC, tetracycline; TCBPE, tetramethyl 4′,4‴,4⁗,4⁗′-(ethene-1,1,2,2-tetrayl)tetrakis([1,1′-biphenyl]-4-carboxylate); TPE, tetraphenylethylene; TPE-Z, quaternized tetraphenylethene salt; ZAIS QDs, Zn–Ag–In–S quantum dots; Zn-BTEC, zinc based metal–organic framework of pyromellitic acid.

food safety issues (Yue et al., 2022). The allowable limit of melamine in infant formula is 20.0 μM (2.5 ppm) in the United States and 8.0 μM (1 ppm) in China (Radhika & Gorthi, 2019). A fluorescence lateral flow assay (LFA) was developed for melamine detection using 6-Aza-2-thiothymine-AuNCs (ATT-AuNCs) based on the AIE effect (Yue et al., 2022). The aggregation-induced fluorescence of ATT-AuNCs was positively correlated with the concentration of melamine, which was triggered upon sample migration to the detection area. Aggregation-induced fluorescence recognition was integrated into LFA technology to avoid the employment of antibodies, aptamers, and other elements, and to minimize background interference. A linear relationship was found between fluorescence enhancement efficiency and the logarithm of melamine concentration from 0.5 to 200 μM with an LOD of 45 nM, which was comparable to that of ELISA. Li, He et al. (2019) used MIP as the recognition part in AIE-based sensors for detecting rhodamine 6G in food samples (dried papaya) and achieved a wide linear range of 0.0–10.0 μmol/L with R^2 of 0.999. Compared with the standard method, this strategy only required simple pretreatment (grinding, extraction, and centrifugation), and the MIP–AIE sensors exhibited excellent performance in real food samples (the recoveries ranged from 96.7% to 103.3%). Furthermore, Na et al. (2019) fabricated SiQDs probed for $K_4[Fe(CN)_6]$ detection in table salt and salted foods based on the ACQ effect of SiQDs induced by the analytes through electrostatic interaction. Simple pretreatment (soaking and washing) was required for the detection to reduce the interference of the salted food matrices and minimize the adverse impact on the detection performance. This research obtained a wide linear range from 0.05 to 8.0 μg/mL, and the detection limit was far lower than the maximum residue limit (10 mg/kg in China and the EU, 1 mg/kg in the United States) in the table salt industry.

Therefore, both ACQ/AIE-based sensors are helpful tools for food additives detection, and the results were considered to be satisfying in complex food matrices. Compared with standard methods, the aggregate-based sensors possessed higher response speed and easy operation, making them ideal platforms for food additives' real-time monitoring.

4.2 | Pesticides

Pesticides play an important role in agriculture in promoting productivity and product quality, but most pesticides are carcinogenic and difficult to degrade in organs, causing accumulation in organs for a long time and serious damage to human health (Huang, Sun, Pu, Wei, Luo, & Wang, 2019; Reeves et al., 2019). Up to now, the standard methods for pesticides generally include high-performance liquid chromatography (HPLC), gas/liquid chromatography, and antibody-related methods. Although these methods are highly sensitive and reliable, the disadvantages of a time-consuming process, expensive instruments, or complicated procedures limit their practical application (Mohapatra et al., 2018). Therefore, AIE/ACQ-based fluorescence sensors have been applied in the pesticides detection field to promote development.

Cai et al. (2020) combined self-assembled MnO_2–AuNCs–SiO_2 nanocomposites with ALP and ascorbic acid for organophosphorus pesticide (OP) detection, and the linear range was from 1 μg/L to 50 mg/L with a detection limit of 0.4 μg/L. Compared with standard methods, the results can be easily observed by the color change and fluorescence alteration, making it possible to realize the in situ imaging detection for pesticide residues on vegetable surfaces. Using non-thiolate DNA–AuNCs as the fluorescent probe, Lu et al. (2018) constructed a sensor of chlorpyrifos, based on the ACQ effect of DNA–AuNCs induced by the hydrolysis of chlorpyrifos, with the detection limit of 0.50 μM, and could be applied to detect chlorpyrifos in real samples with simple pretreatment (the recoveries in different spiked concentrations were ranged from 97.1% to 105.4%). In addition, the sensor could be extended to detect the other OPs with a similar structure as chlorpyrifos. Compared to the immunochromatography method, the proposed strategy exhibited the merits of cost-effectiveness and a wide range of applications but the weakness of being time-consuming (1 h for fluorescence response) and relative insensitivity. Mohapatra et al. (2018) designed an atrazine detection strategy based on the AIE effect, using a highly fluorescent CD as a fluorophore and surface amine groups as receptors to recognize, which worked efficiently over a broad linear concentration range (5 pmol/L to 7 nmol/L) with an LOD of 3 pmol/L, which was lower than the maximum admissible limits (0.01–0.5 mg/kg in the EU, 3 mg/kg in the United States, and 0.05 mg/kg in China) for vegetables. The proposed strategy exhibited high speed (20 min) and low detection limit and reliable analytical performance in real samples (recoveries range from 97% to 100%) with simple pretreatment. Jiao et al. (2018) developed a new biosensor based on aptamer-CD nanoaggregates for acetamiprid detection, according to the principle that acetamiprid could disturb the aptamer-induced ACQ effect of CDs and recover the fluorescence. The sensor provided a linear range from 0.2 to 20 ng/L for acetamiprid with an LOD of 0.04 ng/L in an aqueous buffer that was far lower than the maximum admissible limits (0.05 mg/kg in the EU, 0.2 mg/kg in the United States) for fruit and vegetable. This sensor can be used for sensing acetamiprid in complex food samples with satisfactory results, but the pretreatment required many

steps, which extended testing time and complicated the procedures.

In general, the low detection limits of aggregate-based sensors make them useful in pesticide detection. Moreover, it is their merits of easy operation and low cost that contributes to their popularity compared to traditional methods. Due to the excellent fluorescence property of the AIE phenomenon, the AIE-based sensors can realize in situ imaging detection for pesticide residues in vegetable surfaces, which exhibit great application potential in the real food industry.

4.3 | Veterinary drugs

In general, veterinary drugs and their metabolites may leave residues in animal products, such as milk, eggs, and meat, causing risks to consumers. Owing to these side effects, multiple methods have been established for veterinary drug detection, including mass spectrometry (MS), HPLC, as well as antibody-related methods (Zhang et al., 2018). In general, these strategies require professional skills, sophisticated equipment, and time-consuming sample pretreatment procedures, limiting their practical application (Esmaelpourfarkhani et al., 2020). In response to this problem, aggregate-based sensors have been applied to monitor veterinary drugs (Hu, Liu, et al., 2020).

Li, Shi et al. (2021) developed red fluorescent CDs for the determination of tetracycline antibiotics, including tetracycline, oxytetracycline, and chlortetracycline, because CDs showed a remarkable AIE phenomenon after the addition of tetracycline antibiotics. For tetracycline, oxytetracycline, and chlortetracycline, this method exhibited high sensitivity with the limits of detection of 12, 23, and 25 nmol/L, respectively, making it useful to detect the tetracycline antibiotics residues in milk product with simple pretreatment (recoveries were in the range of 93.4%–107.6%). Owning to the excellent photostability, low cytotoxicity, and the simple synthesis of the red fluorescent CDs, the proposed method demonstrated higher practical feasibility compared to other fluorescence sensors. Zhang et al. (2018) successfully developed an aptamer-based fluorescent biosensor for chloramphenicol detection based on an AIE probe and GO, exhibiting high sensitivity toward chloramphenicol with a detection limit of 0.36 ng/mL. Compared to the standard method HPLC, the proposed strategy exhibited excellent analytical performance, including comparable sensitivity, easy operation, low cost, and rapidity. Using AIEFMs as the label, Wang, Hu et al. (2019) established a competitive lateral flow immunoassay for sulfamethazine detection with a corresponding linear range of 0.05–5 ng/mL and an LOD of 0.028 ng/mL, which was lower than the maximum admissible limits for animal originated products at 100 μg/kg in the EU and 100–200 μg/kg in the United States. The high fluorescence intensity and broad excitation–emission spectrum of AIEFM endowed the method with higher sensitivity compared to other lateral flow immunoassays. In the meantime, Hu, Liu et al. (2020) employed AIEFM in lateral flow immunoassay for norfloxacin detection in nine types of animal-derived food. The application of AIEFM significantly improves the limitation of lateral flow immunoassays, such as sensitivity and poor matric tolerance. The sensors had been used to detect norfloxacin in 135 real samples from honey, egg, chicken, milk, beef, lamb, fish, pig liver, and pork after simple pretreatment with detection limit values of 0.03, 0.03, 0.02, 0.04, 0.14, 0.30, 0.15, 0.04, and 0.22 ng/mL, which were below the maximum admissible limits in animal originated products at 0.1–1.0 mg/kg in the United States and 0.1 mg/kg in the EU. The sensitivity was compatible with HPLC–MS/MS in detecting norfloxacin. The merits of rapidity, anti-interference, and convenience made the proposed method suitable for the detection of norfloxacin in different real samples.

In summary, the high sensitivity of aggregate-based sensors makes them suitable for actual requirements of veterinary drug residue detection in food products. In the meantime, aggregate-based sensors are regarded as promising tools for real-time detection due to their high efficiency and convenient operation. The combination of immunoassay endows the sensors with attractive properties of remarkable selectivity and anti-interference, contributing to reliable results in multiple complex food matrices of the sensing system.

4.4 | Mycotoxins

Mycotoxins are highly toxic secondary metabolites produced by various fungi that may occur naturally in food, causing a severe threat to human and animal health (Huang, Sun, Pu, & Wei, 2019; Yang et al., 2020). Recently, HPLC and ELISA have been adopted for mycotoxin detection. However, HPLC methods often require complicated pretreatment and sophisticated instrumentation, whereas ELISA methods can meet the challenge of unstable antibodies but are highly expensive. Owning to these concerns, many studies have focused on mycotoxin detection using AIE/ACQ-based fluorescence sensors.

Especially, AFB_1 is of wide concern due to its strongest carcinogenesis in humans and animals. The allowable limit of AFB_1 for grains and peanuts is 20 μg/kg in the United States, 2–4 μg/kg in the EU, and 5–10 μg/kg in China. Zhao, Yang et al. (2019) used an intrinsic conformational response-leveraged aptamer probe for AFB_1

detection based on the synergetic utilization of AIE and FRET effects. Due to the introduction of the FRET process, the sensor exhibited high sensitivity with a detection limit of 0.29 ng/mL, which was lower than the maximum admissible limit and allowed to one-pot, mix-to-read detection of AFB_1 at room temperature within 1 min. The proposed strategy has been applied in real samples (bean paste, peanut oil, triturated corn, soil, and tap water) detection after simple pretreatment (extraction and dilution) with recovery values in the range of 91.8%–111.1%. Compared to ELISA, the proposed method exhibited higher stability, faster response, and lower expense, which was well fit for on-site detection. By adopting DNA polymerization, the sensitivity of aggregate-based aptasensors for AFB_1 can be further improved. Wang, Zheng et al. (2019) proposed a novel aggregate–based aptasensor using ACQ dyes, AuNPs/DNA composites, and MNPs, which was applied in maize samples with a reliable result compared to HPLC. Because of the employment of the DNA polymerization technique, more ACQ dyes were assembled on the AuNPs/DNA composites with significant fluorescence quenching, exhibiting high sensitivity toward AFB_1, with a detection limit of 3.1 pg/mL. However, more time had to be consumed during the adoption of this strategy, and the procedures were considered to be complicated, limiting the practical application. The aggregation inducing a color change of AuNP is remarkable and can be easily observed through the naked eye, making AuNP considered to be a promising fluorescence material in the development of cheap "point-of-care" platforms. Chen et al. (2018) reported a detection method for fumonisin B_1 based on direct competitive plasmonic ELISA and AuNP aggregation induced by a horseradish peroxidase/H_2O_2/tyramine system, to construct an on-site detection platform for real food samples. This method exhibited a color change from deep blue to red with a cutoff limit of 12.5 ng/mL observed by the naked eye and has been applied in corn samples with good accuracy and robustness (the recoveries were in the range of 76.5%–96.7%). The proposed method exhibited excellent agreement with the conventional ELISA and HPLC methods. Zhang, Duan et al. (2020) constructed an AIE-based sensor for the patulin (PAT) toxin by applying strand displacement amplification and DNA G-quadruplex, achieving signal amplification to obtain a detection limit of 0.042 pg/mL (far below the maximum admissible limit, which is 50 μg/kg for jam in the United States and the EU, and 25 μg/kg for fruits in the EU and China) with a wider linear range of 0.001–100 ng/mL. Owning to strand displacement amplification and excellent fluorescence property of AIEgens, the aptasensors demonstrated outstanding sensitivity, easier operation, and shorter testing time (1 h) compared to HPLC. The proposed method has been used to detect PAT in grape/apple juice with good accuracy (recoveries of 97.8%–105.3%), and pretreatment was required. First, PAT was extracted from the samples, and then, the solvent was removed to avoid an adverse impact on the detection performance. Although the pretreatment required many steps, it was simpler compared with the standard method HPLC, showing the excellent performance of the proposed sensors. The label-free and turn-on analysis for ochratoxin A (OTA) could be realized by applying AIE dyes in an aptamer biosensor that possessed high sensitivity with a detection limit of 0.4 ng/mL (the maximum residue limit for wine at 2 ng/mL in the EU, 0.5 μg/L in the United States, and 2 μg/kg in China), convenience, easy operation, and rapidity (45 min). The specificity of aptasensor contributed to the excellent performance of OTA analysis in wine and coffee, indicating their potential in practical detection for food safety control (Zhu et al., 2019). Pretreatment was conducted to reduce the interference from food samples as wine and coffee were diluted with methanol–water followed by shaking and centrifuging to obtain supernatant for further detection. The procedures were relatively simple, further indicating the merits of convenience.

To sum up, aptamer recognition units have been generally used in aggregate-based mycotoxin sensors due to their remarkable selectivity, stability, and high adaptability with AIE/ACQ-active molecules. Owning to the participation of aptamers, the sensitivity of aggregate-based sensors was comparable with HPLC methods. In the meantime, the excellent fluorescence property of AIE/ACQ materials endowed the sensors with the merits of fast response and obvious color change, which are suitable for real-time food safety monitoring.

4.5 | Pathogens

Bacterial contamination in food is a major public health threat to humans due to the infections and diseases produced by harmful microorganisms (Esua, Cheng, & Sun, 2021a; Wang, Pu, & Sun, 2018). Several methods have been applied for bacteria detection, such as specimen culturing, polymerase chain reaction, and target-specific immunoassays. However, they usually required long incubation duration, complicated procedures, and expensive costs. Due to the merits of rapidity, sensitivity, and convenience, aggregate-based fluorescence sensors become a promising tool for the reliable monitoring of foodborne pathogens (Guo et al., 2020; Huang, Sun, Wu, Pu, & Wei, 2021; Wu, Pu, & Sun, 2019).

A water-soluble near-infrared emissive luminogen with AIE characteristics, namely, TTVP, has been applied for ultrafast Gram-positive bacteria discrimination

(Lee et al., 2020). TTVP could selectively distinguish Gram-positive bacteria from Gram-negative bacteria through a washing-free procedure after only a 3 s incubation period. Positively charged TTVP gathered around negatively charged bacterial surfaces due to electrostatic interaction, but TTVP insertion would be hindered by the complicated structure of Gram-negative bacteria, making the discrimination only effective for Gram-positive bacteria. Esua, Cheng, & Sun, 2021b However, with prolonged incubation time (about 5 min), Gram-negative bacteria *Escherichia coli* would also be stained with TTVP, exerting an adverse effect on the accuracy of the proposed method. Besides, some researchers were devoted to developing aggregate-based sensors that only targeted a certain range of bacterial species. Ajish et al. (2018) studied AIE properties of glucosyacrylamides for *E. coli* detection, indicating that the interaction between glycoacrylamides and the protein FimH of *E. coli* triggered the transformation of glucosyacrylamides into aggregates with the fluorescence emission. The linear range of this sensor was 1.00×10^6 – 1.70×10^8 cells/mL with an LOD of 7.30×10^5 cells/mL. Although the detection limit of *E. coli* was higher than the maximum admissible limit in food products, the proposed method significantly reduced the testing time to 1 h and simplified the operation procedures, exhibiting great potential in food safety hazard monitoring for unprocessed meat or sea products. Zhang, Xu et al. (2019) applied AIEFM as a probe in the immunochromatographic assay for *E. coli* O157:H7 with a detection limit of 3.98×10^3 CFU/mL, which was 10 times lower than conventional FMs. In the meantime, this method exhibited excellent specificity and fast response, which was able to distinguish *E. coli* O157:H7 from *E. coli* within 25 min. Guo et al. (2020) combined an aptamer and an antibody with AIEgens (aptamer-MNPs and IgG-TPE-OH@BSA NPs) to establish a promising *L. monocytogenes* detection method with a detection range of 10–10^6 CFU/mL, and a low LOD of 10 CFU/mL. Compared to ELISA, this method requires no pre-enrichment or washing during the detection process, and the testing time was around 90 min. Due to the anti-interference ability, the method was applied in real sample detection (water and pork meat) with simple pretreatment (grinding and soaking) to obtain pork leachate for further detection, and the average recoveries are located between 95.37% and 101.90%. As an extension of MIPs, bacteria-imprinted polymers have been applied in the AIE sensor for *S. aureus* rapid and specific detection with a detection limit as low as 6.9 CFU/mL (Guo et al., 2022). The participation of bacteria-imprinted polymers endowed the proposed sensor with high stability and specificity, facilitating the excellent rapid detection in complex food matrices with high recovery rates from 99.6% to 102.7%. Compared to ELISA, this strategy exhibited higher sensitivity, easier procession, and better stability.

Generally speaking, AIEgens themselves still remain a challenge to identify specific bacteria species, and their sensitivity was unable to meet the requirement of food safety hazard detection. The employment of aptamer, antibody, and MIP recognition units significantly improved the detection performance of *E. coli*, *S. aureus*, or *L. monocytogenes* bacteria, which revealed great development prospects in aggregate-based bacteria rapid detection.

4.6 | Metal cations

Certain metal cations are necessary for basic functions in the life process, but they can cause serious toxic damage to human health; thus, the accurate quantitation of metal cations is crucial in food safety control. Several methods have been constructed for metal cation detection, including atomic absorption spectrometry (AAS), inductively coupled plasma, and immunochromatography. However, some defects are existing in these methods, such as expensive equipment needed, complex preprocessing, and tedious operation routine. The advantages of aggregate-based fluorescence sensors attracted many researchers in the field of metal cation quantitation (Wang, Bai, et al., 2020).

Zou et al. (2020) designed water-soluble ZnO QDs modified with (3-aminopropyl) triethoxysilane (APTEs) for Cu^{2+} determination with a detection limit of 1.72 nmol/L, which was quite lower than standard (2 mg/L) for drinking water set by WHO and comparable with the detection limit of standard method AAS. In the meantime, the proposed method simplified the procedures of the detection and reduced the expense, meeting the requirement for actual detection. The sensor has only been applied to detect Cu^{2+} in drinking water with simple pretreatment (chlorine removing and boiling), so the ability of anti-interference in complex food matrices was unclear. Using TSA-capped ZnS QDs, Kayal and Halder (2019) created a splendid method with a detection limit for soluble arsenic down to a few ppb levels ((0.79 ± 0.01 ppb for As(III) and 2.79 ± 0.02 ppb for As(V)), which was below the maximum contaminant level (10 μg/L by WHO). The proposed strategy was extremely selective using the fluorescence turn-on principle without any interruption from any other coexisting ions in an aquatic system. Moreover, the method has the potential to be adopted in real sample detection (local pond water), with recovery rates ranging from 97.6% to 102.6%. Wang, Bai et al. (2020) developed 4-chlorothiophenol capped CuNCs for Hg(II) sensing because the AIE fluorescence of CuNCs could be quenched by Hg(II) due to aggregates destruction, which exhibited

a linear response ranging from 1 to 500 nmol/L with an LOD of 0.3 nmol/L, which was more sensitive than the AAS method. The sensors could be implemented in a test strip (which underwent a color change from red to blue) to facilitate visual determination of Hg(II) in complex environmental water samples with good recoveries of 98.5%–103%. The proposed strategy would be a useful tool for Hg(II) real-time monitoring. Yi et al. (2023) synthesized sodium alginate–based hydrogel doped with TPE derivatives to develop an AIE hydrogel sensor for Hg(II) detection with an LOD of 0.01206 mg/kg, which was lower than FAO/WHO standard. The proposed hydrogel was coated on different carriers for the visual and adaptive detection of Hg-contaminated seafood, exhibiting high potential in on-site food safety screening due to merits of storage stability, rapidity (15 min), and accuracy (recoveries ranged from 90% to 114%). Wei et al. (2019) developed a fluorescent Cd^{2+} probe based on the AIE of ZAIS QDs due to the interaction between Cd^{2+} and QDs, exhibiting a broad detection range from 25 μmol/L to 2 mmol/L and an LOD of 1.56 μmol/L. The method was successfully applied to the determination of Cd^{2+} in water samples (pond water and tap water) with recoveries between 98.1% and 103.3%, and the detection process only took 20 min. Introducing aptamer into an Ag NCs fluorescence system, Zhang and Wei (2018) investigated the detection of Pb^{2+}, which demonstrated high accuracy and reliability in real water samples (relative standard deviation was in the range of 0.47%–0.92%). The proposed probe possessed low toxicity and high sensitivity, achieving an LOD of 3.0 nmol/L, and a linear range from 5 to 50 nmol/L, which was comparable with standard methods. Chen et al. (2019) developed an AIE-based supramolecular polymer gel, by introducing multiple self-assembly driving forces, for multiple metal cation analyzation with signal amplification. The gel could ultra-sensitively detect the multiple heavy metal ions (Hg^{2+}, Cu^{2+}, and Fe^{3+}) with detection limits of 0.126, 0.0929, and 0.100 nmol/L, respectively, which is comparable to the AAS method. In the meantime, the supramolecular polymer gel can be transformed into thin films as an ideal platform for convenient heavy metal ion monitoring, but the performance in real samples was not evaluated in the research.

All in all, if the target samples are real water samples (drinking water or environmental water), the number of metal ions will be accurately determined by aggregate-based sensors even without recognition units. However, if the detection is supposed to perform in complex food matrices, the interferents from food will exert an adverse effect on the sensors. Up to now, the study of the feasibility of aggregate-based metal ion sensors in real food matrices is still insufficient and requires more attention.

5 | IMPROVEMENT STRATEGIES

When researchers devoted themselves to improving the sensitivity, selectivity, and practicability of aggregate-based fluorescence sensor and their applications in food hazard detection, several strategies have been adopted.

First, advanced materials have been applied as AIE/ACQ fluorophores or as fluorescence intensifiers. Ti_3C_2 MXene nanosheets are regarded as promising candidates for their fluorescence sensors because of exciting properties, such as surface hydrophilicity and rich surface chemistry. Applying Ti_3C_2 MXene nanosheets significantly endowed the ACQ-based sensor with rapidity, high sensitivity, and selectivity compared with other fluorescence sensors as well as standardized detection procedures. The present method showed good accuracy and precision for the simultaneous fluorescence detection of Ag^+ and Mn^{2+} ions in food and water samples (Desai et al., 2019). Supramolecular brush polymers were modified with ACQ-active fluorophores to detect Cu^{2+} with remarkable sensitivity because the brush structure could promote the coordination with targeted metal ions (Liu et al., 2021). The inherent properties of microporosity, high loading capacity, and confinement effect make MOFs become preferable materials to construct AIE-based sensors. MOFs could help to significantly improve the stability and emission intensity of CuNCs as well as endow them with selective fluorescence response toward analytes (Gao et al., 2020).

Second, establishing a ratiometric sensor is always considered to be an effective way to boost sensitivity and efficiency. Several studies combined other fluorescent materials with aggregate-based sensors to achieve dual emission. CDs and SiNPs were excellent candidates for providing reference signals in aggregate-based sensors, as their fluorescence intensity stayed still during aggregation (Fu et al., 2020; Qu, Huang, et al., 2018). After combining the internal reference, the probe exhibited obvious fluorescent color variation, which could be easily recognized. Rare-earth elements also could be introduced in aggregate-based sensors as another fluorescence signal to respond to the concentration change of the analytes, which endowed the sensor with highly sensitive, excellently selective, and high response speed (2 min) (Shen, Wei, Chen, et al., 2022). Researchers also rationally employed specific fluorophores, which excitation spectra largely overlapped with the emission spectra of AIEgen, into aggregate-based sensors, using the FRET process to generate dual emission (Li, He, et al., 2019; Zhao, Yang, et al., 2019). The FRET process further leverages the response signal, consequently, dramatically increasing the sensitivity of probes. Some of the other researchers cooperated AIEgens with

ACQ-active fluorophores; in this way, another ratiometric aggregate-based sensor could be constructed (Xu, Chen, et al., 2018).

Third, researchers made progress in elevating the selectivity and stability of the recognition units. Guo et al. (2022) constructed an *N*-Succinyl-Chitosan doping bacteria-imprinted composite film, extending MIPs to bacteria-imprinted polymers. Compared with antibodies, bacteria-imprinted polymers were more stable and easier to operate, making this film able to detect *S. aureus* as low as 6.9 CFU/mL when combined with AIEgens. On the other hand, Guo et al. (2020) simultaneously introduced antibody and aptamer units to first establish aggregate-based specific *L. monocytogenes* sensors that required no pre-enrichment or washing during the detection process. Aptamers were responsible for specifically capturing *L. monocytogenes*, whereas AIEgens labeled antibodies further improved the selectivity, enabling the sensor to have LOD as low as 10 CFU/mL.

Above all, the development of ratiometric sensors, advanced materials, and recognition units are solutions or strategies to address the improvement required for the detection. Stability can be improved by the introduction of MIPs for bacteria detection or MOFs for seafood freshness evaluation. Selectivity can be elevated by the employment of Ti_3C_2 MXene nanosheets for Ag^+ and Mn^{2+} ions detection. Sensitivity can be enhanced by the application of a supramolecular brush polymer sensor for Cu^{2+} and a combination of FRET for AIE-based AFB_1 sensors. Rapidity can be boosted by the incorporation of rare-earth elements for AIE tetracycline sensors, whereas expense can be reduced by the construction of wash-free detection strategies for bacteria using antibodies and aptamers. Through comprehensively understanding the mechanism and behavior of AIE/ACQ-activated materials, researchers chose these suitable strategies for improvement.

6 | CHALLENGES AND FUTURE WORK

Despite great advances in aggregate-based fluorescence sensors in food hazard detection, there are still challenging issues that should be solved for their future developments, indicating that more effort should be made in the future.

- Future work can focus on the structure modification of AIEgens to approach controllable aggregation. Structure modification of fluorescent materials affects the solubility, fluorescence intensity, and wavelength of their aggregates, making them more suitable as signal parts for sensitive and selective detection. Especially for organic molecules with AIE-active, many studies focused on the ingenious molecular structure design to endow the molecules with advantageous characteristics. However, accurate molecular structure designs are challenging. For example, cationization and ionization can change the aggregation degree of the materials and increase their solubility in water, whereas carboxylation or hydroxylation endows the aggregates with hydrophily. Long-chain alkylation makes the aggregates unconfined and reduces the water solubility, whereas increasing the conjugated system of AIE molecules can increase the emission wavelength, light capture ability, and fluorescence yield but reduces the water solubility. The result of AIE-active organic molecules design may be used as a reference for the modification of other fluorescence materials such as ligands-capped MNCs and QDs in future studies.
- Advanced statistical techniques can help to improve aggregate-based sensors. In general, the aggregation degree of fluorescent materials is correlated linearly with the concentration of analytes, which is the fundamental mechanism for establishing aggregate-based quantitative sensors. The structure of analytes also affects the aggregation degree and fluorescence change, which has been applied for analyte distinguishment. However, the diversity of aggregation degrees and fluorescence changes induced by different analytes is a challenge, which still requires much attention. Accurate identification may be achieved by applying advanced statistical techniques (such as machine learning) because the artificial neural network can analyze the unique fluorescence change processes and use it for distinguishment, which can be an area in future studies.
- More efforts can be made to increase the analyte diversity of aggregate-based sensors. The introduction of recognition units widens the range of analytes of aggregate-based sensors, making the detection targets beyond just ions or simple organic molecules. However, it is still a challenge to fulfill the practical needs of food hazard detection, expanding the types of sensing targets is important. The targets for bioimaging can also be applied as indicators for food hazard detection. For instance, the number of fungi can be evaluated through mitochondria targeting, and the freshness of aquatic products can be assessed through ATP detection (Gao et al., 2020; Kulik et al., 2020). Advanced technology can be combined with aggregate-based sensors. For instance, hyperspectral imaging can be applied to capture the tiny change of fluorescence emission in the sensing system, whereas microneedle patches can be employed to gather microscale analytes rapidly.
- The application of frequently used recognition units requires further consideration. Although the recognition units can remarkably improve the accuracy of aggregate-based sensors, the high cost and tedious

operation hinder their way to practical application. Finding cheap, stable, and accessible recognition units and introducing them into sensors is a challenging issue for aggregate-based assays. Both enzymes and glycosyl have recognition capabilities and are easier to generate, and more studies can thus be performed in future for constructing such sensors.

- Future work can make more effort on the application of aggregate-based sensors in bacteria rapid detection. Recent studies have reported several methods for microbial detection but still remained some imperfections (Bai et al., 2021). First, lots of studies could not make a clear distinction between Gram-positive or Gram-negative bacteria because they applied AIEgens staining time to distinguish these two classes of bacteria, which seemed uncontrollable in practice, lack of sensitivity, and would be interrupted by the microenvironment of bacteria. Therefore, using aggregate-based sensors to identify certain bacterial species, especially Gram-negative bacteria, can be an area for future work. Further work can examine the biochemical characteristics of bacteria and their metabolite for creating new recognition strategies and increasing the identifiable bacteria. Second, bacteria can be packed together by self-secreted extracellular polymeric substances (EPS) to form biofilms. Because of EPS, AIEgens will be difficult to penetrate the biofilms to interact with bacteria inside which further decrease the detection efficiency and accuracy. Therefore, the existence of foodborne bacteria biofilm makes it difficult to realize in situ bacteria detection on food surfaces or inert contact surfaces of food processing facilities, limiting the development of techniques for bacteria contamination real-time monitoring in the food industry. Further work can work on to construct an aggregate-based bacterial biosensor that can resist the adverse effect of biofilms during detection. Combining the aggregate-based biosensor with functional units for penetration or biofilm adherence inhibition might be a helpful way.
- On the one hand, the aggregate-based fluorescence sensors exhibited comparable sensitivity and selectivity, higher convenience, and easier operation compared to standard methods. On the other hand, the characteristics of low expense, fast response, and visuality endowed the sensors with remarkable potential in the field of real-time, in situ rapid detection in the food industry. So far, it is still at the preliminary stage of utilizing aggregate-based fluorescence sensors in practical laboratories for food analysis, and the standardized methods, commercial kits, and equipment were insufficient, but plenty of studies focused on promoting the practical application. AIE/ACQ probes were implemented in a paper, fiber cotton, electrospun as well as hydrogel by researchers to construct point-of-care tools for food safety monitoring. With the aid of visual detection with a smartphone, the AIE/ACQ sensing systems can be a rapid screening method for issues with food safety, which was widely acknowledged that promising tools for food safety analysis (Shen, Wei, Zhu et al., 2022). Aggregate-based sensors can be designed as on-package labels in various forms. Despite directly adding to the already prepared detecting system, the form of aggregate-based fluorescence sensors in food hazard detection can become more variable to reach the practical need for food safety monitoring in different scenarios. Researchers used MNC aggregates and AIE polymers to construct a solid-phase packaging label; volatile biogenic amine gas generated from seafood can directly quench the fluorescence of AIE through an electron transfer mechanism (Liu et al., 2022; Zhang, Ma, et al., 2022). More and more research studies focus on the construction of on-package label based on these sensors to visually detect food freshness and safety in real time; however, developing stable, sensitive, harmless labels are still challenging.
- Food matrices are complex in nature, and different nutrients might affect fluorescence results, exerting adverse influence on the detecting performance of the aggregate-based sensors. Such an issue requires addressing in future research. One strategy is to minimize the interaction between real-food samples and aggregate-based sensors by only detecting the volatile gas generated from real food. Most research concentrated on the detection of volatile biogenic amines or H_2S for freshness monitoring. Future research may devote to broadening the detectable food-related volatile gas, for example, volatile ethylene, and aromatic hydrocarbon can be applied to monitor the ripeness of fruits. The second strategy is employing specific recognition units in the aggregate-based sensors to elevate their selectivity. Despite aptamer, antibody, molecular imprinting, and host–guest recognition units mentioned above, researchers work on broadening the kinds of recognition units, including enzymes, carbohydrate, peptide, and peptidomimetic polymers (Li, Chen, et al., 2021; Vishwakarma et al., 2021). Moreover, separating the recognition process and fluorescence process might be helpful to deal with this issue, similar to the study of Guo et al. (2022). The target *S. aureus* can be precisely captured by the imprinted film, followed by rinsing with water twice to get rid of irrelevant substances, and then, the film would be reacted with AuNPs to provide a corresponding fluorescence signal. These principles might inspire future studies to prevent the interruption of real food products.
- Another problem that hindered the development of aggregate-based fluorescence sensors for food safety

monitoring was the poor characterization of the stability of the new material. To be used routinely, the batches of new materials should have appropriate stability to be included in commercial kits. However, in general, reports on new materials and their application usually disregard the evaluation of the stability. Given the facts above, stability assessment and improvement are highly required. The introduction of MOFs might be useful to elevate the stability of fluorescence signal, whereas MIP or aptamers will be more stable than frequently used antibodies as a recognition unit. Such materials will be attracted more attention in the future studied.

Overall, since the discovery of the AIE effect, aggregate-based fluorescence sensors have received great attention and have been developed prosperously. It is thus expected that aggregate-based sensors should become a new generation of sensing technology for food safety and quality control in the foreseeable future.

7 | CONCLUSIONS

Fluorescent materials (often modified by hydroxyl, carboxyl, thiol, or amino groups) participate in aggregate-based fluorescence sensors with high sensitivity through different strategies. Generally speaking, these strategies include analytes triggering the aggregation of fluorescence materials; analytes destroying the aggregates of fluorescence materials; analytes decomposing the AIE quencher and resuming the emission; and analytes reducing the solubility of fluorescence materials. However, these strategies alone can only be used for detecting a limited range of analytes, which mainly include metal cations, anions, and small organic molecules (some antibiotics or pesticides) with simple structures, because analytes with similar structures (such as with the same functional groups or electronegativity) can stimulate the aggregation of the same material. Recognition units include aptamer, antibody, molecular imprinting, and host–guest recognition can combine with the aggregate-based fluorescence sensor to make further progress in detection sensitivity and range of analytes (such as mycotoxins, pathogens, and complex organic molecules). Moreover, due to the advantages of aggregate-based fluorescence sensing technology, it is boomingly used in the food hazard detection field, including mycotoxins, pathogens, food additives, pesticides, veterinary drugs, and metal cation detection.

AUTHOR CONTRIBUTIONS

Zhuoyun Chen: Writing – original draft; conceptualization; investigation. **Ji Ma**: Conceptualization; investigation. **Da-Wen Sun**: Funding acquisition; writing – review & editing; supervision; resources.

ACKNOWLEDGEMENTS

The authors are grateful to the National Natural Science Foundation of China (3217161084) for its support. This research was also supported by the Guangzhou Key Laboratory for Intelligent Sensing and Quality Control of Agricultural Products (202102100009), the Guangdong Provincial Science and Technology Plan Projects (2020A1414010160), the Guangdong Basic and Applied Basic Research Foundation (2022A1515012489, 2020A1515010936), the Contemporary International Collaborative Research Centre of Guangdong Province on Food Innovative Processing and Intelligent Control (2019A050519001), and the Common Technical Innovation Team of Guangdong Province on Preservation and Logistics of Agricultural Products (2023KJ145).

Open access funding provided by IReL.

CONFLICT OF INTEREST STATEMENT

All authors declare that they have no conflicts of interest.

ORCID

Da-Wen Sun https://orcid.org/0000-0002-3634-9963

REFERENCES

Ajish, J. K., Ajish Kumar, K. S., Ruhela, A., Subramanian, M., Ballal, A. D., & Kumar, M. (2018). AIE based fluorescent self assembled glycoacrylamides for *E. coli* detection and cell imaging. *Sensors and Actuators B: Chemical*, *255*, 1726–1734.

Bai, H., He, W., Chau, J. H. C., Zheng, Z., Kwok, R. T. K., Lam, J. W. Y., & Tang, B. Z. (2021). AIEgens for microbial detection and antimicrobial therapy. *Biomaterials*, *268*, 120598.

Beatty, M. A., & Hof, F. (2021). Host-guest binding in water, salty water, and biofluids: General lessons for synthetic, bio-targeted molecular recognition. *Chemical Society Reviews*, *50*, 4812–4832.

BelBruno, J. J. (2019). Molecularly imprinted polymers. *Chemical Reviews*, *119*, 94–119.

Borse, S., Murthy, Z. V. P., & Kailasa, S. K. (2020). Chicken egg white mediated synthesis of platinum nanoclusters for the selective detection of carbidopa. *Optical Materials*, *107*, 110085.

Cai, M., Ding, C., Wang, F., Ye, M., Zhang, C., & Xian, Y. (2019). A ratiometric fluorescent assay for the detection and bioimaging of alkaline phosphatase based on near infrared Ag_2S quantum dots and calcein. *Biosensors & Bioelectronics*, *137*, 148–153.

Cai, Y., Qiu, Z., Lin, X., Zeng, W., Cao, Y., Liu, W., & Liu, Y. (2020). Self-assembled nanomaterials based on aggregation-induced emission of AuNCs: Fluorescence and colorimetric dual-mode biosensing of organophosphorus pesticides. *Sensors and Actuators B: Chemical*, *321*, 128481.

Capoferri, D., Della Pelle, F., Del Carlo, M., & Compagnone, D. (2018). Affinity sensing strategies for the detection of pesticides in food. *Foods*, *7*, 148.

Chabok, A., Shamsipur, M., Yeganeh-Faal, A., Molaabasi, F., Molaei, K., & Sarparast, M. (2019). A highly selective semiconducting polymer dots-based "off-on" fluorescent nanoprobe for iron, copper and histidine detection and imaging in living cells. *Talanta*, *194*, 752–762.

Chen, H., Wang, S., Fu, H., Chen, F., Zhang, L., Lan, W., Yang, J., Yang, X., & She, Y. (2020). A colorimetric sensor array for

recognition of 32 Chinese traditional cereal vinegars based on "turn-off/on" fluorescence of acid-sensitive quantum dots. *Spectrochimica Acta Part A—Molecular and Biomolecular Spectroscopy*, *227*, 117683.

Chen, J., Wang, Y., Wei, X., Liu, Z., Xu, F., Li, H., & He, X. (2021). A novel "turn-off" fluorescence assay based on acid-copper nanoclusters in deep eutectic solvent micelles for co-aggregation inducing fluorescence enhancement and its application. *Talanta*, *223*, 121731.

Chen, L., Cheng, Z., Luo, M., Wang, T., Zhang, L., Wei, J., Wang, Y., & Li, P. (2021). Fluorescent noble metal nanoclusters for contaminants analysis in food matrix. *Critical Reviews in Food Science and Nutrition*, 1–19.

Chen, X., Liang, Y., Zhang, W., Leng, Y., & Xiong, Y. (2018). A colorimetric immunoassay based on glucose oxidase-induced AuNP aggregation for the detection of fumonisin B1. *Talanta*, *186*, 29–35.

Chen, Y. Y., Gong, G. F., Fan, Y. Q., Zhou, Q., Zhang, Q. P., Yao, H., Zhang, Y. M., Wei, T. B., & Lin, Q. (2019). A novel AIE-based supramolecular polymer gel serves as an ultrasensitive detection and efficient separation material for multiple heavy metal ions. *Soft Matter*, *15*, 6878–6884.

Chini, M. K., Kumar, V., Javed, A., & Satapathi, S. (2019). Graphene quantum dots and carbon nano dots for the FRET based detection of heavy metal ions. *Nano-Structures & Nano-Objects*, *19*, 100347.

Chowdhury, P., Banerjee, A., Saha, B., Bauri, K., & De, P. (2022). Stimuli-responsive aggregation-induced emission (AIE)-active polymers for biomedical applications. *ACS Biomaterials Science & Engineering*, *8*, 4207–4229.

Chu, H., Yao, D., Chen, J., Yu, M., & Su, L. (2020). Double-emission ratiometric fluorescent sensors composed of rare-earth-doped ZnS quantum dots for $Hg^{(2+)}$ detection. *ACS Omega*, *5*, 9558–9565.

Chungchai, W., Amatatongchai, M., Meelapsom, R., Seebunrueng, K., Suparsorn, S., & Jarujamrus, P. (2019). Development of a novel three-dimensional microfluidic paper-based analytical device (3D-?PAD) for chlorpyrifos detection using graphene quantum-dot capped gold nanocomposite for colorimetric assay. *International Journal of Environmental Analytical Chemistry*, *100*, 1160–1178.

Desai, M. L., Basu, H., Singhal, R. K., Saha, S., & Kailasa, S. K. (2019). Ultra-small two dimensional MXene nanosheets for selective and sensitive fluorescence detection of Ag^{+} and Mn^{2+} ions. *Colloids and Surfaces A: Physicochemical and Engineering Aspects*, *565*, 70–77.

Dong, J., Li, X., Zhang, K., Di Yuan, Y., Wang, Y., Zhai, L., Liu, G., Yuan, D., Jiang, J., & Zhao, D. (2018). Confinement of aggregation-induced emission molecular rotors in ultrathin two-dimensional porous organic nanosheets for enhanced molecular recognition. *Journal of the American Chemical Society*, *140*, 4035–4046.

Esmaelpourfarkhani, M., Abnous, K., Taghdisi, S. M., & Chamsaz, M. (2020). A novel turn-off fluorescent aptasensor for ampicillin detection based on perylenetetracarboxylic acid diimide and gold nanoparticles. *Biosensors & Bioelectronics*, *164*, 112329.

Esua, O. J., Cheng, J. H., & Sun, D.-W. (2020). Antimicrobial activities of plasma-functionalized liquids against foodborne pathogens on grass carp (Ctenopharyngodon Idella). *Applied Microbiology and Biotechnology*, *104*, 9581–9594.

Esua, O. J., Cheng, J. H., & Sun, D.-W. (2021a). Novel technique for treating grass carp (Ctenopharyngodon idella) by combining plasma functionalized liquids and Ultrasound: Effects on bacterial inactivation and quality attributes. *Ultrasonics Sonochemistry*, *76*, 105660.

Esua, O. J., Cheng, J. H., & Sun, D.-W. (2021b). Optimisation of treatment conditions for reducing Shewanella putrefaciens and Salmonella Typhimurium on grass carp treated by thermoultrasound-assisted plasma functionalized buffer. *Ultrasonics Sonochemistry*, *76*, 105609.

Fu, Y., Wu, S., Zhou, H., Zhao, S., Lan, M., Huang, J., & Song, X. (2020). Carbon dots and a CdTe quantum dot hybrid-based fluorometric probe for spermine detection. *Industrial & Engineering Chemistry Research*, *59*, 1723–1729.

Gan, Z., Hu, X., Huang, X., Li, Z., Zou, X., Shi, J., Zhang, W., Li, Y., & Xu, Y. (2021). A dual-emission fluorescence sensor for ultrasensitive sensing mercury in milk based on carbon quantum dots modified with europium (III) complexes. *Sensors and Actuators B: Chemical*, *328*, 128977.

Gao, T., Sun, D.-W., Tian, Y., & Zhu, Z. (2021). Gold–silver core-shell nanorods based time-temperature indicator for quality monitoring of pasteurized milk in the cold chain. *Journal of Food Engineering*, *306*, 110624.

Gao, M., & Tang, B. Z. (2017). Fluorescent sensors based on aggregation-induced emission: Recent advances and perspectives. *ACS Sensors*, *2*(10), 1382–1399.

Gao, X., Liu, J., Zhuang, X., Tian, C., Luan, F., Liu, H., & Xiong, Y. (2020). Incorporating copper nanoclusters into a zeolitic imidazole framework-90 for use as a highly sensitive adenosine triphosphate sensing system to evaluate the freshness of aquatic products. *Sensors and Actuators B: Chemical*, *308*, 127720.

Ge, S., He, J., Ma, C., Liu, J., Xi, F., & Dong, X. (2019). One-step synthesis of boron-doped graphene quantum dots for fluorescent sensors and biosensor. *Talanta*, *199*, 581–589.

Guo, Y., Zhao, C., Liu, Y., Nie, H., Guo, X., Song, X., Xu, K., Li, J., & Wang, J. (2020). A novel fluorescence method for the rapid and effective detection of *Listeria monocytogenes* using aptamer-conjugated magnetic nanoparticles and aggregation-induced emission dots. *Analyst*, *145*, 3857–3863.

Guo, Y., Zheng, Y., Liu, Y., Feng, X., Dong, Q., Li, J., Wang, J., & Zhao, C. (2022). A concise detection strategy of *Staphylococcus aureus* using N-Succinyl-Chitosan-dopped bacteria-imprinted composite film and AIE fluorescence sensor. *Journal of Hazardous Materials*, *423*, 126934.

Halawa, M. I., Wu, F., Nsabimana, A., Lou, B., & Xu, G. (2018). Inositol directed facile "green" synthesis of fluorescent gold nanoclusters as selective and sensitive detecting probes of ferric ions. *Sensors and Actuators B: Chemical*, *257*, 980–987.

He, H., Sun, D.-W., Wu, Z., Pu, H., & Wei, Q. (2022). On-off-on fluorescent nanosensing: Materials, detection strategies and recent food applications. *Trends in Food Science & Technology*, *119*, 243–256.

He, W., Zheng, Z., Bai, H., Xiong, L. H., Wang, L., Li, Y., Kwok, R. T. K., Lam, J. W. Y., Hu, Q., Cheng, J., & Tang, B. Z. (2021). A biocompatible dual-AIEgen system without spectral overlap for quantitation of microbial viability and monitoring of biofilm formation. *Materials Horizons*, *8*, 1816–1824.

Hong, Y., Lam, J. W., & Tang, B. Z. (2011). Aggregation-induced emission. *Chemical Society Reviews*, *40*, 5361–5388.

Hu, B., Sun, D.-W., Pu, H., & Wei, Q. (2020). A dynamically optical and highly stable pNIPAM@ Au NRs nanohybrid substrate for sensitive SERS detection of malachite green in fish fillet. *Talanta*, *218*, 121188.

Hu, R., Leung, N. L., & Tang, B. Z. (2014). AIE macromolecules: Syntheses, structures and functionalities. *Chemical Society Reviews*, *43*, 4494–4562.

Hu, R., Qin, A., & Tang, B. Z. (2020). AIE polymers: Synthesis and applications. *Progress in Polymer Science*, *100*, 101176.

Hu, S., Liu, J., Zhang, G., Wang, Z., Xiao, X., Li, D., Peng, J., & Lai, W. (2020). Reliable performance of aggregation-induced emission nanoparticle-based lateral flow assay for norfloxacin detection in nine types of animal-derived food. *Talanta*, *219*, 121245.

Huang, H., Li, M., Hao, M., Yu, L., & Li, Y. (2021). A novel selective detection method for sulfide in food systems based on the GMP-Cu nanozyme with laccase activity. *Talanta*, *235*, 122775.

Huang, L., Sun, D.-W., Pu, H., & Wei, Q. (2019). Development of nanozymes for food quality and safety detection: Principles and recent applications. *Comprehensive Reviews in Food Science and Food Safety*, *18*, 1496–1513.

Huang, L., Sun, D.-W., Pu, H., Wei, Q., Luo, L., & Wang, J. (2019). A colorimetric paper sensor based on the domino reaction of acetylcholinesterase and degradable ?-MnOOH nanozyme for sensitive detection of organophosphorus pesticides. *Sensors and actuators B: chemical*, *290*, 573–580.

Huang, L., Sun, D.-W., Wu, Z., Pu, H., & Wei, Q. (2021). Reproducible, shelf-stable, and bioaffinity SERS nanotags inspired by multivariate polyphenolic chemistry for bacterial identification. *Analytica Chimica Acta*, *1167*, 338570.

Huang, L., Sun, D.-W., & Pu, H. (2022). Photosensitized peroxidase mimicry at the hierarchical 0D/2D heterojunction-like quasi metal-organic framework interface for boosting biocatalytic disinfection. *Small*, *18*, 2200178.

Huang, X. L., Guo, Q., Zhang, R. Y., Zhao, Z., Leng, Y. K., Lam, J. W. Y., Xiong, Y. H., & Tang, B. Z. (2020). AIEgens: An emerging fluorescent sensing tool to aid food safety and quality control. *Comprehensive Reviews in Food Science and Food Safety*, *19*, 2297–2329.

Huang, Y. Q., Zhang, X., Xue, J. H., Liu, L., Chen, S. H., & Wang, Y. S. (2020). Sensitive and selective assay of uranyl based on the aggregation induced fluorescent quenching of protamine capped gold nanoclusters. *Spectrochimica Acta Part A: Molecular and Biomolecular Spectroscopy*, *226*, 117649.

Jia, J., Xu, W., Yu, Y., Fu, Y., He, Q., Cao, H., & Cheng, J. (2019). A selective and stepwise aggregation of a new fluorescent probe for dinitrate explosive differentiation by self-adaptive host-guest interaction. *Science China Chemistry*, *63*, 116–125.

Jia, Y., Wu, F., Liu, P., Zhou, G., Yu, B., Lou, X., & Xia, F. (2019). A label-free fluorescent aptasensor for the detection of aflatoxin B1 in food samples using AIEgens and graphene oxide. *Talanta*, *198*, 71–77.

Jiao, Z., Zhang, H., Jiao, S., Guo, Z., Zhu, D., & Zhao, X. (2018). A turn-on biosensor-based aptamer-mediated carbon quantum dots nanoaggregate for acetamiprid detection in complex samples. *Food Analytical Methods*, *12*, 668–676.

Kayal, S., & Halder, M. (2019). A ZnS quantum dot-based super selective fluorescent chemosensor for soluble ppb-level total arsenic [As(III) + As(V)] in aqueous media: Direct assay utilizing aggregation-enhanced emission (AEE) for analytical application. *Analyst*, *144*, 3710–3715.

Kulik, T., Bilska, K., & Żelechowski, M. (2020). Promising perspectives for detection, identification, and quantification of plant pathogenic fungi and oomycetes through targeting mitochondrial DNA. *International Journal of Molecular Sciences*, *21*, 2645.

Lee, M. M. S., Xu, W., Zheng, L., Yu, B., Leung, A. C. S., Kwok, R. T. K., Lam, J. W. Y., Xu, F. J., Wang, D., & Tang, B. Z. (2020). Ultrafast discrimination of Gram-positive bacteria and highly efficient photodynamic antibacterial therapy using near-infrared photosensitizer with aggregation-induced emission characteristics. *Biomaterials*, *230*, 119582.

Li, D., Chen, J., Hong, M., Wang, Y., Haddleton, D. M., Li, G.-Z., & Zhang, Q. (2021). Cationic glycopolymers with aggregation-induced emission for the killing, imaging, and detection of bacteria. *Biomacromolecules*, *22*, 2224–2232.

Li, D., Chen, J., Xu, X., Bao, C., & Zhang, Q. (2020). Supramolecular assemblies of glycoclusters with aggregation-induced emission for sensitive phenol detection. *Chemical Communications*, *56*, 13385–13388.

Li, H., Guo, Z., Xie, W., Sun, W., Ji, S., Tian, J., & Lv, L. (2019). A label-free fluorometric aptasensor for adenosine triphosphate (ATP) detection based on aggregation-induced emission probe. *Analytical Biochemistry*, *578*, 60–65.

Li, K., Wang, L., Chen, J., Yan, M., Fu, Y., He, Q., & Cheng, J. (2021). Detecting methylphenethylamine vapor using fluorescence aggregate concentration quenching materials. *Sensors and Actuators B: Chemical*, *334*, 129629.

Li, L., Shi, L., Jia, J., Eltayeb, O., Lu, W., Tang, Y., Dong, C., & Shuang, S. (2021). Red fluorescent carbon dots for tetracycline antibiotics and pH discrimination from aggregation-induced emission mechanism. *Sensors and Actuators B: Chemical*, *332*, 129513.

Li, R., Liu, Q., Jin, Y., & Li, B. (2019). Fluorescent enzyme-linked immunoassay strategy based on enzyme-triggered in-situ synthesis of fluorescent copper nanoclusters. *Sensors and Actuators B: Chemical*, *281*, 28–33.

Li, S., Xu, W., Huang, Z., & Jia, Q. (2022). Anchoring Cu nanoclusters on melamine-formaldehyde microspheres: A new strategy for triggering aggregation-induced emission toward specific enzyme-free methyl parathion sensing. *Journal of Agricultural and Food Chemistry*, *70*(45), 14522–14530.

Li, Y., He, W., Peng, Q., Hou, L., He, J., & Li, K. (2019). Aggregation-induced emission luminogen based molecularly imprinted ratiometric fluorescence sensor for the detection of Rhodamine 6G in food samples. *Food Chemistry*, *287*, 55–60.

Li, Y., Hou, L., Shan, F., Zhang, Z., Li, Y., Liu, Y., Peng, Q., He, J., & Li, K. (2019). A novel aggregation-induced emission luminogen based molecularly imprinted fluorescence sensor for ratiometric determination of rhodamine B in food samples. *ChemistrySelect*, *4*, 11256–11261.

Li, Y., Xi, W., Hussain, I., Chen, M., & Tan, B. (2021). Facile preparation of silver nanocluster self-assemblies with aggregation-induced emission by equilibrium shifting. *Nanoscale*, *13*, 14207–14213.

Liang, B., & Han, L. (2020). Displaying of acetylcholinesterase mutants on surface of yeast for ultra-trace fluorescence detection of organophosphate pesticides with gold nanoclusters. *Biosensors & Bioelectronics*, *148*, 111825.

Lin, Q., Guan, X. W., Fan, Y. Q., Wang, J., Liu, L., Liu, J., Yao, H., Zhang, Y. M., & Wei, T. B. (2019). A tripodal supramolecular sensor to successively detect picric acid and CN^- through guest competitive controlled AIE. *New Journal of Chemistry*, *43*, 2030–2036.

Ling, Y., Wang, L., Zhang, X. Y., Wang, X. H., Zhou, J., Sun, Z., Li, N. B., & Luo, H. Q. (2020). Ratiometric fluorescence detection of dopamine based on effect of ligand on the emission of Ag nanoclusters and aggregation-induced emission enhancement. *Sensors and Actuators B: Chemical*, *310*, 127858.

Liu, G., Huang, X., Zheng, S., Li, L., Xu, D., Xu, X., Zhang, Y., & Lin, H. (2018). Novel triadimenol detection assay based on fluorescence resonance energy transfer between gold nanoparticles and cadmium telluride quantum dots. *Dyes and Pigments*, *149*, 229–235.

Liu, H., Wang, Y., Mo, W., Tang, H., Cheng, Z., Chen, Y., Zhang, S., Ma, H., Li, B., & Li, X. (2020). Dendrimer-based, high-luminescence conjugated microporous polymer films for highly sensitive and selective volatile organic compound sensor arrays. *Advanced Functional Materials*, *30*(13), 1910275.1–1910275.7.

Liu, J., Gan, L., & Yang, X. (2020). Glutenin-directed gold nanoclusters employed for assaying vitamin B1. *New Journal of Chemistry*, *44*, 487–491.

Liu, Q., Wang, H., Han, P., & Feng, X. (2019). Fluorescent aptasensing of chlorpyrifos based on the assembly of cationic conjugated polymer-aggregated gold nanoparticles and luminescent metal-organic frameworks. *Analyst*, 144.

Liu, S., Wu, Q., Zhang, T., Zhang, H., & Han, J. (2021). Supramolecular brush polymers prepared from 1,3,4-oxadiazole and cyanobutoxy functionalised pillar[5]arene for detecting $Cu^{(2+)}$. *Organic & Biomolecular Chemistry*, *19*, 1287–1291.

Liu, X., Wang, Y., Zhang, Z., Zhu, L., Gao, X., Zhong, K., Sun, X., Li, X., & Li, J. (2022). On-package ratiometric fluorescent sensing label based on AIE polymers for real-time and visual detection of fish freshness. *Food Chemistry*, *390*, 133153.

Lu, F., Yang, H., Tang, Y., Yu, C. J., Wang, G., Yuan, Z., & Quan, H. (2020). 11-Mercaptoundecanoic acid capped gold nanoclusters with unusual aggregation-enhanced emission for selective fluorometric hydrogen sulfide determination. *Mikrochimica Acta*, *187*, 200.

Lu, N., Ma, J., & Sun, D.-W. (2022). Enhancing physical and chemical quality attributes of frozen meat and meat products: Mechanisms, techniques and applications. *Trends in Food Science & Technology*, *124*, 63–85.

Lu, Q., Zhou, T., Wang, Y., Gong, L., & Liu, J. (2018). Transformation from gold nanoclusters to plasmonic nanoparticles: A general strategy towards selective detection of organophosphorothioate pesticides. *Biosensors & Bioelectronics*, *99*, 274–280.

Lv, L., Cui, C., Xie, W., Sun, W., Ji, S., Tian, J., & Guo, Z. (2019). A label-free aptasensor for turn-on fluorescent detection of ochratoxin A based on aggregation-induced emission probe. *Methods and Applications in Fluorescence*, *8*, 015003.

Ma, X., Sun, R., Cheng, J., Liu, J., Gou, F., Xiang, H., & Zhou, X. (2015). Fluorescence aggregation-caused quenching versus aggregation-induced emission: A visual teaching technology for undergraduate chemistry students. *Journal of Chemical Education*, *93*, 345–350.

Mahato, P., Shekhar, S., Agrawal, S., Pramanik, S., & Mukherjee, S. (2022). Assembly-induced emission in mercaptosuccinic acid-templated silver nanoclusters: Metal ion selectivity and pH sensitivity. *ACS Applied Nano Materials*, *5*, 7571–7579.

Mo, Q., Liu, F., Gao, J., Zhao, M., & Shao, N. (2018). Fluorescent sensing of ascorbic acid based on iodine induced oxidative etching and aggregation of lysozyme-templated silver nanoclusters. *Analytica Chimica Acta*, *1003*, 49–55.

Mohapatra, S., Bera, M. K., & Das, R. K. (2018). Rapid "turn-on" detection of atrazine using highly luminescent N-doped carbon quantum dot. *Sensors and Actuators B: Chemical*, *263*, 459–468.

Mortazavi Moghadam, F., Bigdeli, M., Tamayol, A., & Shin, S. R. (2021). TISS nanobiosensor for salivary cortisol measurement by aptamer Ag nanocluster SAIE supraparticle structure. *Sensors and Actuators B: Chemical*, *344*, 130160.

Na, M., Chen, Y., Han, Y., Ma, S., Liu, J., & Chen, X. (2019). Determination of potassium ferrocyanide in table salt and salted food using a water-soluble fluorescent silicon quantum dots. *Food Chemistry*, *288*, 248–255.

Niu, Z., Liu, Y., Li, X., Zhu, H., Zhang, M., Yan, K., & Chen, H. (2022). Colorimetric detection of sulfamethazine based on target resolved calixarene derivative stabilized gold nanoparticles aggregation. *Mikrochim Acta*, *189*, 71.

Nguyen, D. K., & Jang, C. H. (2022). Ultrasensitive colorimetric detection of amoxicillin based on Tris-HCl-induced aggregation of gold nanoparticles. *Analytical Biochemistry*, *645*, 114634.

Packirisamy, V., & Pandurangan, P. (2021). Heterocyclic thiol protected supramolecular self-assembly of silver nanoclusters for ultrasensitive detection of toxic Hg (II) ions in nanomolar range. *Journal of Molecular Liquids*, *344*, 117769.

Parani, S., & Oluwafemi, O. S. (2020). Selective and sensitive fluorescent nanoprobe based on AgInS2-ZnS quantum dots for the rapid detection of Cr (III) ions in the midst of interfering ions. *Nanotechnology*, *31*, 395501.

Pathan, S., Jalal, M., Prasad, S., & Bose, S. (2019). Aggregation-induced enhanced photoluminescence in magnetic graphene oxide quantum dots as a fluorescence probe for As(III) sensing. *Journal of Materials Chemistry A*, *7*, 8510–8520.

Qu, F., Huang, W., & You, J. (2018). A fluorescent sensor for detecting dopamine and tyrosinase activity by dual-emission carbon dots and gold nanoparticles. *Colloids and Surfaces B—Biointerfaces*, *162*, 212–219.

Qu, F., Zhao, L., Han, W., & You, J. (2018). Ratiometric detection of $Zn^{(2+)}$ and $Cd^{(2+)}$ based on self-assembled nanoarchitectures with dual emissions involving aggregation enhanced emission (AEE) and its application. *Journal of Materials Chemistry B*, *6*, 4995–5002.

Qu, W. J., Yang, H. H., Hu, J. P., Qin, P., Zhao, X. X., Lin, Q., Yao, H., Zhang, Y. M., & Wei, T. B. (2021). A novel bis-acylhydrazone supramolecular gel and its application in ultrasensitive detection of CN? *Dyes and Pigments*, *186*, 108949.

Radhika, N. K., & Gorthi, S. S. (2019). Enhancement of the fluorescence properties of double stranded DNA templated copper nanoparticles. *Materials Science and Engineering: C*, *98*, 1034–1042.

Reeves, W. R., McGuire, M. K., Stokes, M., & Vicini, J. L. (2019). Assessing the safety of pesticides in food: How current regulations protect human health. *Advances in Nutrition*, *10*, 80–88.

Ren, S. H., Liu, S. G., Ling, Y., Shi, Y., Li, N. B., & Luo, H. Q. (2019). Fabrication of silver nanoclusters with enhanced fluorescence triggered by ethanol solvent: A selective fluorescent probe for $Cr^{(3+)}$ detection. *Analytical and Bioanalytical Chemistry*, *411*, 3301–3308.

Saberi, Z., Rezaei, B., & Ensafi, A. A. (2019). Fluorometric label-free aptasensor for detection of the pesticide acetamiprid by using cationic carbon dots prepared with cetrimonium bromide. *Mikrochim Acta*, *186*, 273.

Sahu, D. K., Singha, D., & Sahu, K. (2019). Sensing of iron(III)-biomolecules by surfactant-free fluorescent copper nanoclusters. *Sensing and Bio-Sensing Research*, *22*, 100250.

Sargazi, S., Fatima, I., Hassan Kiani, M., Mohammadzadeh, V., Arshad, R., Bilal, M., Rahdar, A., Diez-Pascual, A. M., & Behzadmehr, R. (2022). Fluorescent-based nanosensors for selective detection of a wide range of biological macromolecules: A comprehensive review. *International Journal of Biological Macromolecules*, *206*, 115–147.

Selvaraj, M., Rajalakshmi, K., Ahn, D. H., Yoon, S. J., Nam, Y. S., Lee, Y., Xu, Y., Song, J. W., & Lee, K. B. (2021). Tetraphenylethene-based fluorescent probe with aggregation-induced emission behavior for $Hg^{(2+)}$ detection and its application. *Analytica Chimica Acta*, *1148*, 238178.

Shen, Y., Wei, Y., Chen, H., Wu, Z., Ye, Y., & Han, D. M. (2022). Liposome-encapsulated aggregation-induced emission fluorogen assisted with portable smartphone for dynamically on-site imaging of residual tetracycline. *Sensors and Actuators B: Chemical*, *350*, 130871.

Shen, Y., Wei, Y., Zhu, C., Cao, J., & Han, D. M. (2022). Ratiometric fluorescent signals-driven smartphone-based portable sensors for onsite visual detection of food contaminants. *Coordination Chemistry Reviews*, *458*, 214442.

Shen, Z., Zhang, C., Yu, X., Li, J., Liu, B., & Zhang, Z. (2019). A facile stage for Cu^{2+} ions detection by formation and aggregation of Cu nanoclusters. *Microchemical Journal*, *145*, 517–522.

Song, Z., Yu, L., Sun, Y., & He, H. (2019). Visual and spectrophotometric detection of metformin based on the host-guest molecular recognition of cucurbit[6]uril-modified silver nanoparticles. *Analytical and Bioanalytical Chemistry*, *411*, 7293–7301.

Su, D., Li, H., Yan, X., Lin, Y., & Lu, G. (2021). Biosensors based on fluorescence carbon nanomaterials for detection of pesticides. *TrAC Trends in Analytical Chemistry*, *134*, 116126.

Sun, D.-W., Huang, L., Pu, H., & Ma, J. (2021). Introducing reticular chemistry into agrochemistry. *Chemical Society Reviews*, *50*, 1070–1110.

Tan, N. D., Lan, C., Yin, J. H., Meng, L., & Xu, N. (2019). Selective detection of trace metronidazole by using a magnetic molecularly imprinted polymer-based fluorescent probe. *Bulletin of the Korean Chemical Society*, *41*, 60–65.

Tang, B. Z., Zhan, X., Gui, Y., Lee, P., Liu, Y., & Zhu, D. (2001). Efficient blue emission from siloles. *Journal of Materials Chemistry*, *11*, 2974–2978.

Tang, L., Xia, J., Zhong, K., Tang, Y., Gao, X., & Li, J. (2020). A simple AIE-active fluorogen for relay recognition of Cu^{2+} and pyrophosphate through aggregation-switching strategy. *Dyes and Pigments*, *178*, 108379.

Tang, Y., Huang, H., Xue, W., Chang, Y., Li, Y., Guo, X., & Zhong, C. (2020). Rigidifying induced fluorescence enhancement in 2D porous covalent triazine framework nanosheets for the simultaneously luminous detection and adsorption removal of antibiotics. *Chemical Engineering Journal*, *384*, 123382.

Vishwakarma, A., Dang, F., Ferrell, A., Barton, H. A., & Joy, A. (2021). Peptidomimetic polyurethanes inhibit bacterial biofilm formation and disrupt surface established biofilms. *Journal of the American Chemical Society*, *143*(25), 9440–9449.

Wan, H., Xu, Q., Gu, P., Li, H., Chen, D., Li, N., He, J., & Lu, J. (2021). AIE-based fluorescent sensors for low concentration toxic ion detection in water. *Journal of Hazardous Materials*, *403*, 123656.

Wang, B., Li, J., Shui, S., & Xu, J. (2021). An acylhydrazone-based AIE organogel for the selective sensing of submicromolar level Al^{3+} and Al(III)-based metallogel formation to detect oxalic acid. *New Journal of Chemistry*, *45*, 1899–1903.

Wang, B., Zheng, J., Ding, A., Xu, L., Chen, J., & Li, C. M. (2019). Highly sensitive aflatoxin B1 sensor based on DNA-guided assembly of fluorescent probe and TdT-assisted DNA polymerization. *Food Chemistry*, *294*, 19–26.

Wang, H. B., Bai, H. Y., Wang, Y. S., Gan, T., & Liu, Y. M. (2020). Highly selective fluorimetric and colorimetric sensing of mercury(II) by exploiting the self-assembly-induced emission of 4-chlorothiophenol capped copper nanoclusters. *Mikrochimica Acta*, *187*, 185.

Wang, K., Pu, H., & Sun, D.-W. (2018). Emerging spectroscopic and spectral imaging techniques for the rapid detection of microorganisms: An overview. *Comprehensive reviews in food science and food safety*, *17*, 256–273.

Wang, Q. B., Zhang, C. J., Yu, H., Zhang, X., Lu, Q., Yao, J. S., & Zhao, H. (2020). The sensitive "turn-on" fluorescence platform of ascorbic acid based on conjugated polymer nanoparticles. *Analytica Chimica Acta*, *1097*, 153–160.

Wang, Z., Hu, S., Zhang, G., Liu, J., Xia, J., Peng, J., & Lai, W. (2019). Aggregation-induced emission-based competitive lateral flow immunoassay for rapid detection of sulfamethazine in honey. *Food and Agricultural Immunology*, *30*, 1303–1317.

Wei, C., Wei, X., Hu, Z., Yang, D., Mei, S., Zhang, G., Su, D., Zhang, W., & Guo, R. (2019). A fluorescent probe for Cd^{2+} detection based on the aggregation-induced emission enhancement of aqueous Zn-Ag-In-S quantum dots. *Analytical Methods*, *11*, 2559–2564.

Wei, D., Li, M., Wang, Y., Zhu, N., Hu, X., Zhao, B., Zhang, Z., & Yin, D. (2023). Encapsulating gold nanoclusters into metal-organic frameworks to boost luminescence for sensitive detection of copper ions and organophosphorus pesticides. *Journal of Hazardous Materials*, *441*, 129890.

Wu, H., & Tong, C. (2019). Nitrogen- and sulfur-codoped carbon dots for highly selective and sensitive fluorescent detection of Hg(2+) ions and sulfide in environmental water samples. *Journal of Agricultural and Food Chemistry*, *67*, 2794–2800.

Wu, L., Pu, H., & Sun, D.-W. (2019). Novel techniques for evaluating freshness quality attributes of fish: A review of recent developments. *Trends in food science & technology*, *83*, 259–273.

Wu, W., Shen, M., Liu, X., Shen, L., Ke, X., & Li, W. (2020). Highly sensitive fluorescence-linked immunosorbent assay based on aggregation-induced emission luminogens incorporated nanobeads. *Biosensors & Bioelectronics*, *150*, 111912.

Xie, S., Liu, Q., Zhu, F., Chen, M., Wang, L., Xiong, Y., Zhu, Y., Zheng, Y., & Chen, X. (2020). AIE-active metal-organic frameworks: Facile preparation, tunable light emission, ultrasensitive sensing of copper(II) and visual fluorescence detection of glucose. *Journal of Materials Chemistry C*, *8*, 10408–10415.

Xu, L., Chen, D., Zhang, Q., He, T., Lu, C., Shen, X., Tang, D., Qiu, H., Zhang, M., & Yin, S. (2018). A fluorescent cross-linked supramolecular network formed by orthogonal metal-coordination and host–guest interactions for multiple ratiometric sensing. *Polymer Chemistry*, *9*, 399–403.

Xu, N., Meng, L., Li, H. W., Lu, D. Y., & Wu, Y. (2018). Polyethyleneimine capped bimetallic Au/Pt nanoclusters are a viable fluorescent probe for specific recognition of

chlortetracycline among other tetracycline antibiotics. *Mikrochimica Acta*, *185*, 294.

Yang, H., Liu, Y., Guo, Z., Lei, B., Zhuang, J., Zhang, X., Liu, Z., & Hu, C. (2019). Hydrophobic carbon dots with blue dispersed emission and red aggregation-induced emission. *Nature Communications*, *10*, 1789.

Yang, Y., Li, G., Wu, D., Liu, J., Li, X., Luo, P., Hu, N., Wang, H., & Wu, Y. (2020). Recent advances on toxicity and determination methods of mycotoxins in foodstuffs. *Trends in Food Science & Technology*, *96*, 233–252.

Ye, C., Wang, Y., Wang, S., & Wang, Z. (2019). Fabrication of cefotaxime sodium-functionalized gold nanoclusters for the detection of copper ions in Chinese herbal medicines. *RSC Advances*, *9*, 5037–5044.

Yi, L., Zhang, Y., Xie, Y., Zhang, X., Jiao, Z., Jiang, G., Chen, H., & Zhang, P. (2023). Portable AIE hydrogel sensor for rapid and visual field detection of heavy metal residue in food. *Dyes and Pigments*, *212*, 111117.

Yin, C., Wu, M., Liu, H., Sun, Q., Sun, X., Niu, N., Xu, J., & Chen, L. (2022). Reversible AIE self-assembled nanohybrids coordinated by La^{3+} for ratiometric visual acid phosphatase monitoring and intracellular imaging. *Sensors and Actuators B: Chemical*, *371*, 132550.

Yin, H. Q., Wang, X. Y., & Yin, X. B. (2019). Rotation restricted emission and antenna effect in single metal-organic frameworks. *Journal of the American Chemical Society*, *141*, 15166–15173.

Yu, W., Li, Y., Xie, B., Ma, M., Chen, C., Li, C., Yu, X., Wang, Z., Wen, K., Tang, B. Z., & Shen, J. (2019). An aggregation-induced emission-based indirect competitive immunoassay for fluorescence "turn-on" detection of drug residues in foodstuffs. *Frontiers in Chemistry*, *7*, 228.

Yuan, Y., Hou, W., Qin, W., & Wu, C. (2021). Recent advances in semiconducting polymer dots as optical probes for biosensing. *Biomaterials Science*, *9*, 328–346.

Yue, X., Pan, Q., Zhou, J., Ren, H., Peng, C., Wang, Z., & Zhang, Y. (2022). A simplified fluorescent lateral flow assay for melamine based on aggregation induced emission of gold nanoclusters. *Food Chemistry*, *385*, 132670.

Zeng, L., Zhu, Z., & Sun, D.-W. (2022). Novel graphene oxide/polymer composite membranes for the food industry: structures, mechanisms and recent applications. *Critical Reviews in Food Science and Nutrition*, *62*, 3705–3722.

Zhang, B., & Wei, C. (2018). Highly sensitive and selective detection of $Pb^{(2+)}$ using a turn-on fluorescent aptamer DNA silver nanoclusters sensor. *Talanta*, *182*, 125–130.

Zhang, C., Huang, L., Sun, D.-W., & Pu, H. (2022). Interfacing metal-polyphenolic networks upon photothermal gold nanorods for triplex-evolved biocompatible bactericidal activity. *Journal of Hazardous Materials*, *426*, 127824.

Zhang, C., Huang, L., Pu, H., & Sun, D.-W. (2021). Magnetic surface-enhanced Raman scattering (MagSERS) biosensors for microbial food safety: Fundamentals and applications. *Trends in Food Science & Technology*, *113*, 366–381.

Zhang, W., Ma, J., & Sun, D.-W. (2021). Raman spectroscopic techniques for detecting structure and quality of frozen foods: principles and applications. *Critical Reviews in Food Science and Nutrition*, *61*, 2623–2639.

Zhang, G., Wang, R., Shi, L., Zhang, C., Zhang, Y., Zhou, Y., Dong, C., Li, G., & Shuang, S. (2019). Aggregation/assembly induced emission based on silk fibroin-templated fluorescent copper nanoclusters for "turn-on" detection of S^{2-}. *Sensors and Actuators B: Chemical*, *279*, 361–368.

Zhang, G. G., Xu, S. L., Xiong, Y. H., Duan, H., Chen, W. Y., Li, X. M., Yuan, M. F., & Lai, W. H. (2019). Ultrabright fluorescent microsphere and its novel application for improving the sensitivity of immunochromatographic assay. *Biosensors & Bioelectronics*, *135*, 173–180.

Zhang, H., Zhao, Z., Turley, A. T., Wang, L., McGonigal, P. R., Tu, Y., Li, Y., Wang, Z., Kwok, R. T. K., Lam, J. W. Y., & Tang, B. Z. (2020). Aggregate science: From structures to properties. *Advanced Materials*, *32*, 2001457.

Zhang, J., Ren, S., Xia, H., Jia, W., & Zhang, C. (2020). AIE-ligand-based luminescent Cd(II)-organic framework as the first "turn-on" Fe^{3+} sensor in aqueous medium. *Journal of Materials Chemistry C*, *8*, 1427–1432.

Zhang, S., Ma, L., Ma, K., Xu, B., Liu, L., & Tian, W. (2018). Label-free aptamer-based biosensor for specific detection of chloramphenicol using AIE probe and graphene oxide. *ACS Omega*, *3*, 12886–12892.

Zhang, W., Ma, J., Sun, D.-W., Cheng, J., Wang, Z., & Tang, B. Z. (2022). An improved ratiometric fluorescent tag based on aggregation-induced emission luminogen for in-situ monitoring of seafood freshness. *Sensors and Actuators B: Chemical*, *373*, 132744.

Zhang, W., Zuo, H., Cheng, Z., Shi, Y., Guo, Z., Meng, N., Thomas, A., & Liao, Y. (2022). Macroscale conjugated microporous polymers: Controlling versatile functionalities over several dimensions. *Advanced Materials*, *34*, 2104952.

Zhang, Y., Duan, B., Bao, Q., Yang, T., Wei, T., Wang, J., Mao, C., Zhang, C., & Yang, M. (2020). Aptamer-modified sensitive nanobiosensors for the specific detection of antibiotics. *Journal of Materials Chemistry*, *8*, 8607–8613.

Zhang, Y., Zhuo, P., Yin, H., Fan, Y., Zhang, J., Liu, X., & Chen, Z. (2019). Solid-state fluorescent carbon dots with aggregation-induced yellow emission for white light-emitting diodes with high luminous efficiencies. *ACS Applied Materials & Interfaces*, *11*, 24395–24403.

Zhao, J., Wang, Z., Lu, Y., Li, H., Guan, Y., Huang, W., & Liu, Y. (2022). Facile and rapid synthesis of copper nanoclusters as a fluorescent probe for the sensitive detection of fluoride ions with the assistance of aluminum. *Dyes and Pigments*, *206*, 110593.

Zhao, X., Kong, D., Jin, R., Li, H., Yan, X., Liu, F., Sun, P., Gao, Y., & Lu, G. (2019). On-site monitoring of thiram via aggregation-induced emission enhancement of gold nanoclusters based on electronic-eye platform. *Sensors and Actuators B: Chemical*, *296*, 126641.

Zhao, Y., Yavari, K., & Liu, J. (2022). Critical evaluation of aptamer binding for biosensor designs. *TrAC Trends in Analytical Chemistry*, *146*, 116480.

Zhao, Z., Yang, H., Deng, S., Dong, Y., Yan, B., Zhang, K., Deng, R., & He, Q. (2019). Intrinsic conformation response-leveraged aptamer probe based on aggregation-induced emission dyes for aflatoxin B1 detection. *Dyes and Pigments*, *171*, 107767.

Zheng, Y., Liu, W., Chen, Y., Li, C., Jiang, H., & Wang, X. (2019). Conjugating gold nanoclusters and antimicrobial peptides: From aggregation-induced emission to antibacterial synergy. *Journal of Colloid and Interface Science*, *546*, 1–10.

Zhou, Y., Zhang, L., Gao, H., Zhu, F., Ge, M., & Liang, G. (2019). Rapid detection of aromatic pollutants in water using swellable micelles

of fluorescent polymers. *Sensors and Actuators B: Chemical*, *283*, 415–425.

Zhu, Y., Xia, X., Deng, S., Yan, B., Dong, Y., Zhang, K., Deng, R., & He, Q. (2019). Label-free fluorescent aptasensing of mycotoxins via aggregation-induced emission dye. *Dyes and Pigments*, *170*, 107572.

Zou, T., Xing, X., Yang, Y., Wang, Z., Wang, Z., Zhao, R., Zhang, X., & Wang, Y. (2020). Water-soluble ZnO quantum dots modified by (3-aminopropyl) triethoxysilane: The promising fluorescent probe for the selective detection of Cu^{2+} ion in drinking water. *Journal of Alloys and Compounds*, *825*, 153904.

How to cite this article: Chen, Z., Ma, J., & Sun, D.-W. (2023). Aggregates-based fluorescence sensing technology for food hazard detection: Principles, improvement strategies, and applications. *Comprehensive Reviews in Food Science and Food Safety*, 1–34. https://doi.org/10.1111/1541-4337.13169